Supplementary Information

Mechanism-Based Allylic Carbasugar Chlorides that form Covalent Intermediates with α-and β-Galactosidases

Oluwafemi Akintola, Sandeep Bhosale,* Andrew J. Bennet*

Department of Chemistry, Simon Fraser University, Burnaby V5A 1S6, British Columbia, Canada.

E-mail: bennet@sfu.ca, sbhosale@sfu.ca

Table of Contents

Enzymatic rate constant and substrate data tables (Tables S1–S6)	S2–S5
Plot for Human α-Galactosidases inactivation by **3** (Figure S1)	S6
Plots for *A. oryzae* β-galactosidase inactivation by **1**–**3** (Figures S2–S4)	S6–S7
Plot for Human α-Galactosidase reactivation (Figure S5)	S8
Mechanism for turnover of **2** and **3** with Human α-galactosidase (Figure S6)	S8
Reaction coordinates for GH27 GalA catalysis (Figure S7)	S9
NMR Spectra (Figures S8–S42)	S10–S44

Table S1: Kinetic Data (percent activity remaining) for Covalent Inhibition of GH27 Human α-galactosidase caused by incubation with **2**.

Time (s)	1 mM	2 mM	3 mM	4 mM	6 mM
60		100.00	100.00	100.00	100.00
180					86.08
240			88.79	86.97	
300	91.74				
360					70.20
420		87.86	75.91		
480				71.04	
600	88.16		65.75		47.54
660		76.83			
780				51.87	
840			53.19		34.35
960		67.12			
1080			43.64	40.14	27.70
1200	75.25				
1380		51.42	32.56		17.48
1560				28.05	
1680					15.83
1740			27.06		
1800	65.65				
1860		37.69			
1926					13.76
2160				19.38	
2340		33.23			9.32
2880		27.81			
3000	49.91				
3900	39.83				

Table S2: Kinetic Data (percent activity remaining) for Covalent Inhibition of GH27 Human α-galactosidase caused by incubation with **3**.

Time (s)	2 mM	3 mM	4 mM	6 mM	8 mM
60		100.00	100.00	100.00	100.00
180				90.48	86.73
240		93.20	89.04		
240					
360				80.45	70.37
420		85.95	81.84		
480	85.47				
540					55.70
600				63.66	
660		74.54	69.40		
720	79.97				44.59
900		67.42	61.00	49.82	
960	75.65				35.63
1200	66.99	59.34			26.75
1260			48.67	37.05	
1500		48.73			21.54
1620			38.42	27.10	
1800	57.70	43.90			
1920					17.72
1980			34.25		
2040	52.34			24.25	
2100		39.15			
2220	48.27				
2400		36.89			
2460	46.54				
2520			29.48	20.62	
3000				18.74	

Table S3: Kinetic Data: rate constants for Covalent Inhibition of GH27 Human α-galactosidase caused by incubation with **2** and **3**.[a]

[I] mM	**2** $10^4 \times k_{obs}$ (s^{-1})	**3** $10^4 \times k_{obs}$ (s^{-1})
1.0	2.5 ± 0.6	ND
2.0	5.2 ± 1.1	3.8 ± 1.5
3.0	8.9 ± 0.9	5.9 ± 1.1
4.0	10.0 ± 0.8	7.7 ± 1.1
6.0	15.0 ± 0.9	10.7 ± 0.7
8.0	ND	14.4 ± 0.6

[a] ND = not determined.

Table S4: Kinetic Data (percent activity regained) following Covalent Inhibition of GH27 Human α-galactosidase caused by incubation with **2** and **3**.

Time (s)	**2**	**3**	Time (s)	**2**	**3**
58.5	15.56	14.51	2975.0	82.93	83.92
150.0	19.39	19.41	3225.0	86.77	84.72
250.0	23.89	24.49	3475.0	90.20	87.81
350.0	30.13	29.12	3725.0	90.75	86.69
450.0	31.08	31.52	3975.0	91.89	90.10
550.0	32.54	41.24	4225.0	92.15	89.19
650.0	36.09	34.77	4475.0	95.67	90.26
750.0	36.17	36.42	4725.0	94.42	96.96
850.0	44.58	46.22	4975.0	92.93	94.73
950.0	48.94	47.13	5225.0	97.27	94.14
1050.0	49.52	49.60	5475.0	97.21	97.87
1150.0	53.07	48.40	5725.0		98.72
1250.0	54.38	51.48	5975.0	98.20	97.39
1350.0	56.99	56.28	6225.0		93.02
1450.0	59.84	60.86	6475.0	97.53	99.68
1550.0	63.83	59.85	6725.0	100.00	97.02
1650.0	63.83	60.12	6975.0		
1725.0	64.03	63.68	7225.0	99.45	98.03
1975.0	69.64	68.32	7475.0		98.56
2225.0	72.67	73.27	7725.0		98.78
2475.0	77.46	75.03	7975.0		100.00
2725.0	80.14	77.05			

Table S5: Kinetic Data: rate constants for GH35 *A. oryzae* β-galactosidase caused by incubation with **1**, **2**, and **3**.[a]

[I] mM	**1** $10^3\times k_{obs}$ (s^{-1})	**2** $10^3\times k_{obs}$ (s^{-1})	**2** $10^3\times k_{obs}$ (s^{-1})
0.1	1.26 ± 0.13	–	–
0.2	1.43 ± 0.16	–	–
0.4	2.63 ± 0.20	5.57 ± 0.06	–
0.5	–	6.22 ± 0.06	–
0.6	3.26 ± 0.21	–	–
0.8	4.51 ± 0.41	11.6 ± 0.1	–
1.0	5.48 ± 0.04	13.2 ± 0.1	1.15 ± 0.01
1.2	6.28 ± 0.50	16.6 ± 0.2	–
1.4	–	16.5 ± 0.2	–
1.8	–	24.1 ± 0.3	–
2.0	–	–	1.96 ± 0.01
3.0	–	–	2.74 ± 0.01
4.0	–	–	3.43 ± 0.02
6.0	–	–	4.23 ± 0.03

Table S6: Kinetic Data (percent activity regained) following Covalent Inhibition of GH35 *A. oryzae* β-galactosidase with **1**, **2**, and **3**.

Time (s)	**1**	**2**	**3**
59			15.30
64	13.44		
150	29.68	31.41	28.86
250	45.11	49.91	47.59
350	57.85	58.69	58.81
450	63.54	64.93	68.62
550	76.89	79.16	
650	80.15	79.94	84.15
750	83.69	85.56	
850	85.82	86.49	92.42
950	90.69	88.50	95.28
1050	90.88	89.74	93.19
1150	95.97	90.46	95.55
1250	94.61	94.69	101.45
1350	97.69	96.85	97.73
1450	97.17	95.46	100.00
1550	94.17	92.63	
1650	94.99	97.94	97.05
1750	98.39	100.00	
1850	100.00	99.23	
1950			101.50

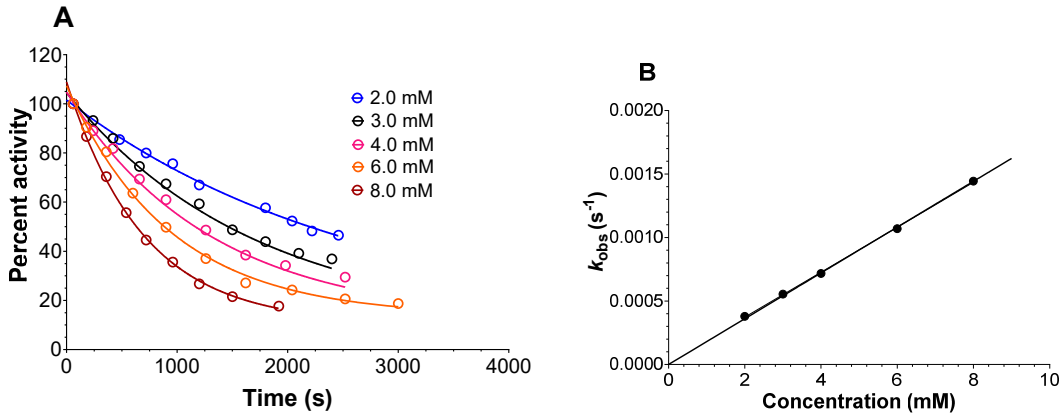


Figure S1: **Covalent Inhibition of GH27 Human α-galactosidase caused by incubation with 3**. (a) First-order loss of enzyme activity due to time-dependent inactivation by different concentrations of **3**, all lines are the least-squares fit to a standard exponential decay. (b) Least squares linear MM plot for the inactivation of GH27 Human α-galactosidase by **3**. All experiments were carried out at T = 37 °C in 50 mM sodium citrate buffer, pH 4.6 containing 50 mM NaCl and 0.1% BSA.

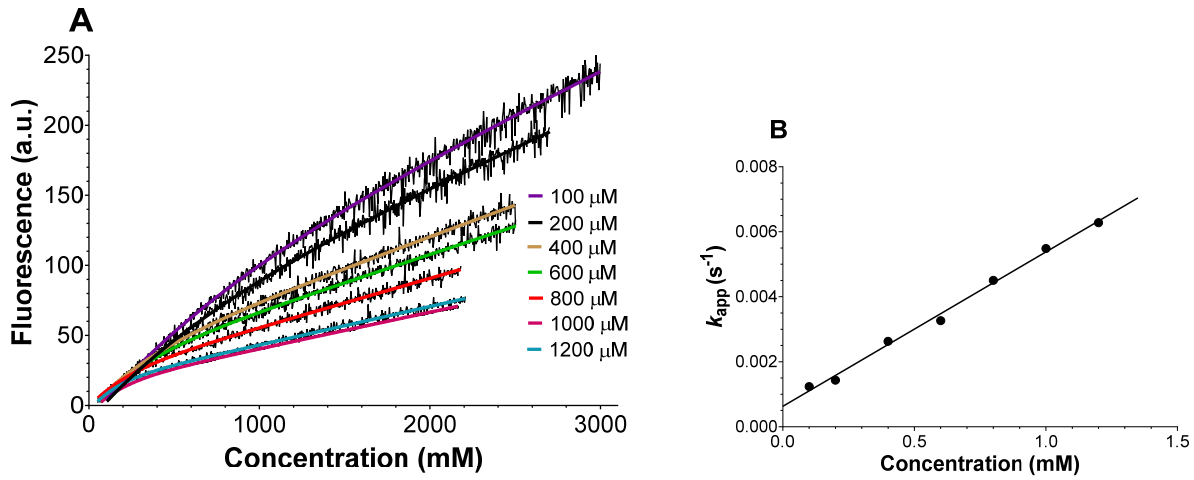


Figure S2: **Covalent Inhibition of GH35 *A. oryzae* β-galactosidase caused by incubation with 1**. (a) First-order loss of enzyme activity due to time-dependent inactivation by different concentrations of **1** in 1 mM 4-methylumbelliferyl β-galactoside. (b) Least squares linear MM plot for the inactivation of *A. oryzae* β-galactosidase by **1**. All experiments were carried out at T = 37 °C in 50 mM sodium acetate buffer, pH 4.5 containing 0.1% BSA.

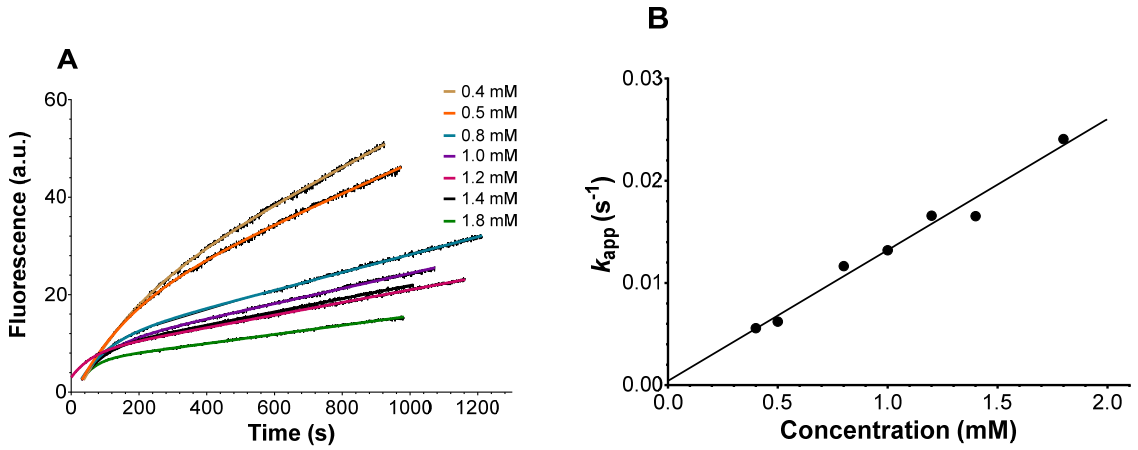


Figure S3: **Covalent Inhibition of GH35 *A. oryzae* β-galactosidase caused by incubation with 2**. (a) First-order loss of enzyme activity due to time-dependent inactivation by different concentrations of **2** in 1 mM 4-methylumbelliferyl β-galactoside. (b) Least squares linear MM plot for the inactivation of *A. oryzae* β-galactosidase by **2**. All experiments were carried out at T = 37 °C in 50 mM sodium acetate buffer, pH 4.5 containing 0.1% BSA.

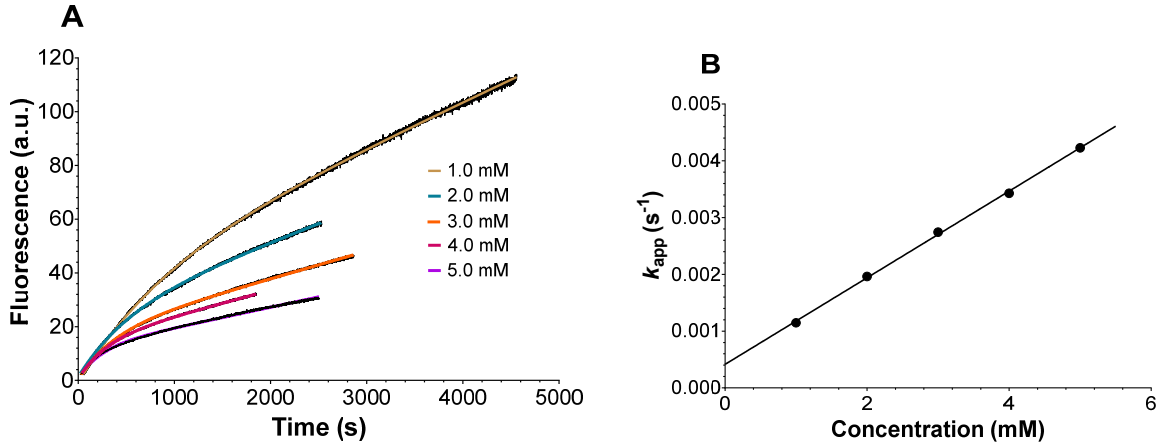


Figure S4: **Covalent Inhibition of GH35 *A. oryzae* β-galactosidase caused by incubation with 3**. (a) First-order loss of enzyme activity due to time-dependent inactivation by different concentrations of **3** in 1 mM 4-methylumbelliferyl β-galactoside. (b) Least squares linear MM plot for the inactivation of *A. oryzae* β-galactosidase by **3**. All experiments were carried out at T = 37 °C in 50 mM sodium acetate buffer, pH 4.5 containing 0.1% BSA.

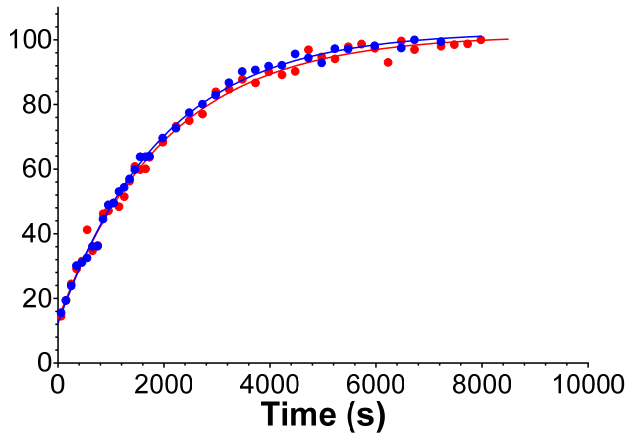


Figure S5: **Reactivation of GH27 Human α-galactosidase after covalent inhibition by 2 and 3**. First-order return of enzyme activity after covalent inhibition by cyclohexenyl-based carbasugars **2** (blue circles) and **3** (red circles), all lines are the least-squares fit to a standard exponential rate law. All experiments were carried out at T = 37 °C in 50 mM sodium citrate buffer, pH 4.6 containing 50 mM NaCl and 0.1% BSA.

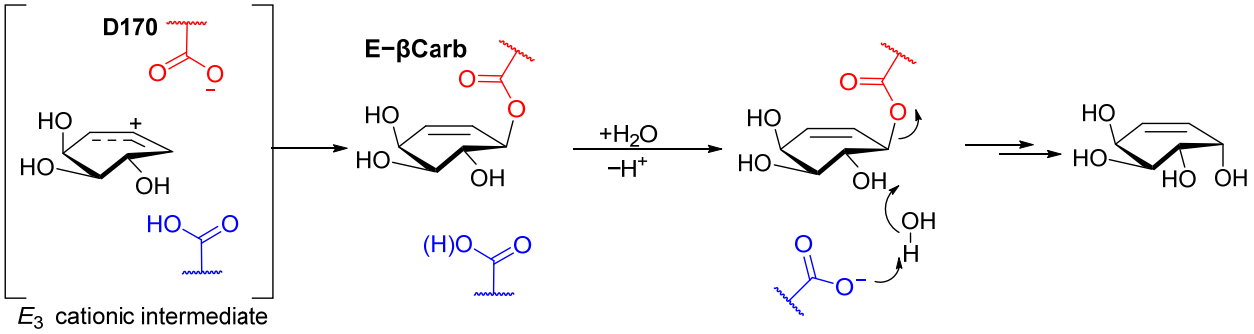


Figure S6: Mechanism for trapping of enzyme bound allylic cation formed from reaction of both **2** and **3** with Human α-galactosidase to give the pseudo-galactosylation intermediate and its subsequent hydrolysis.

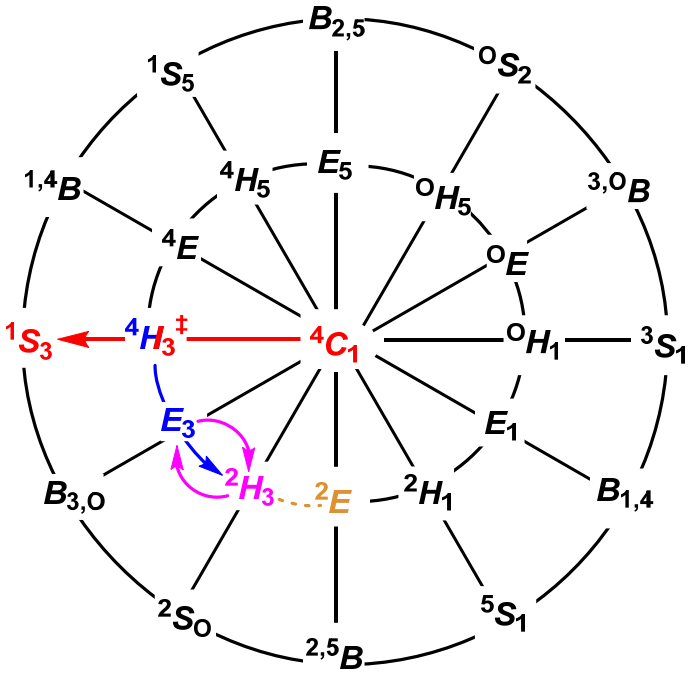


Figure S7. Proposed reaction coordinates for GH27 GalA-catalyzed hydrolysis of natural substrates and covalent inhibition by carbasugars **2** and **3**. Substrate hydrolysis occurs via a $^{4}C_{1}$ Michaelis complex via a $^{4}H_{3}$ half-chair transition state to give a $^{1}S_{3}$ skew boat (red arrow) covalent enzyme intermediate. Allylic carbasugar inhibitor **2** reacts from a $^{4}H_{3}$ via an E_{3} allylic cation to give a $^{2}H_{3}$ or ^{2}E intermediate (blue arrow). While **3** requires a conformational itinerary of a $^{2}H_{3}$ to E_{3} and back to a $^{2}H_{3}$ or ^{2}E (pink arrows).

Figure S8: ^{1}H-NMR spectrum of **1** in CD_3OD (600 MHz).

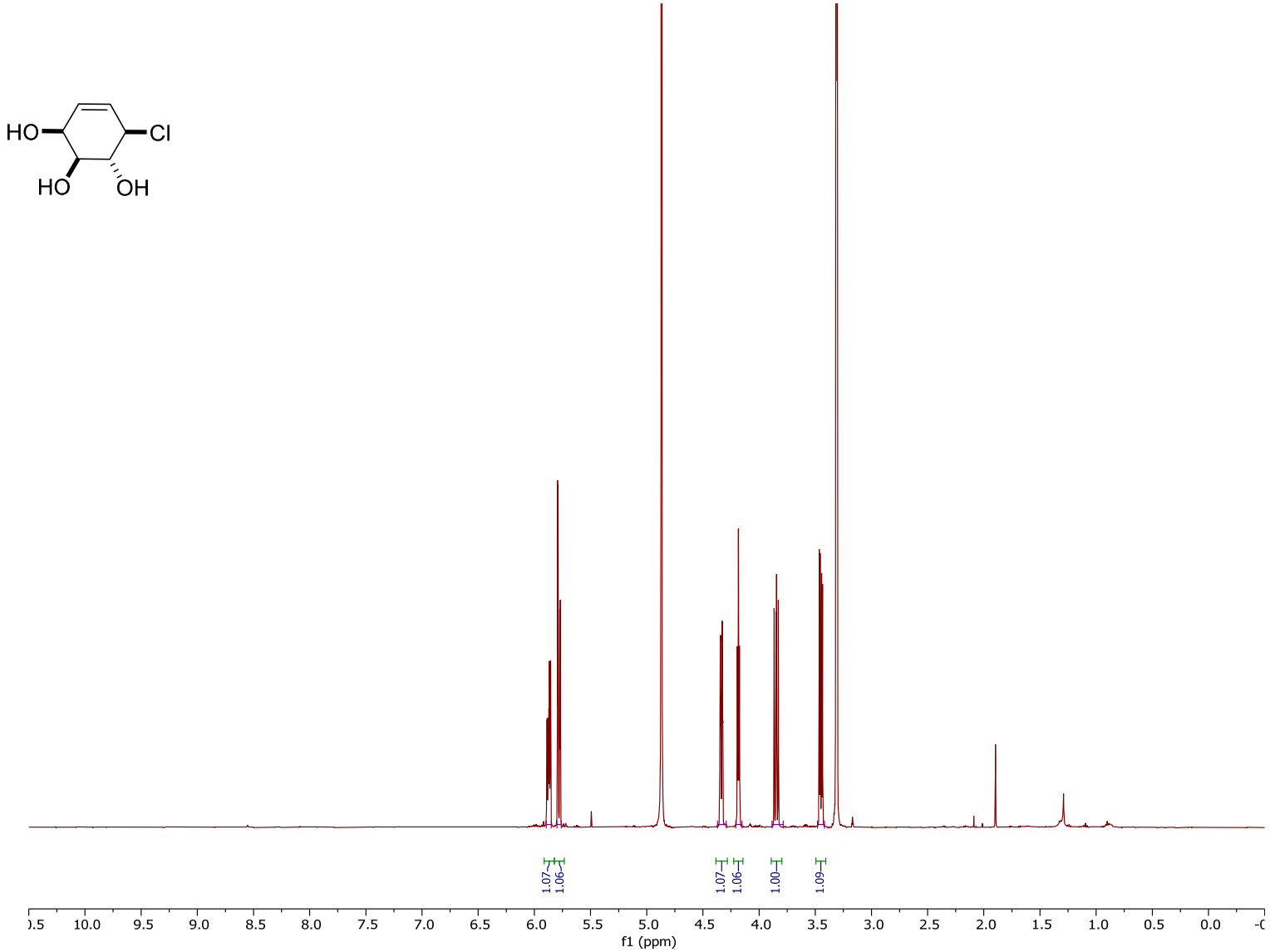


Figure S9: ^{13}C {^{1}H}-NMR spectrum of **1** in CD_3OD (151 MHz).

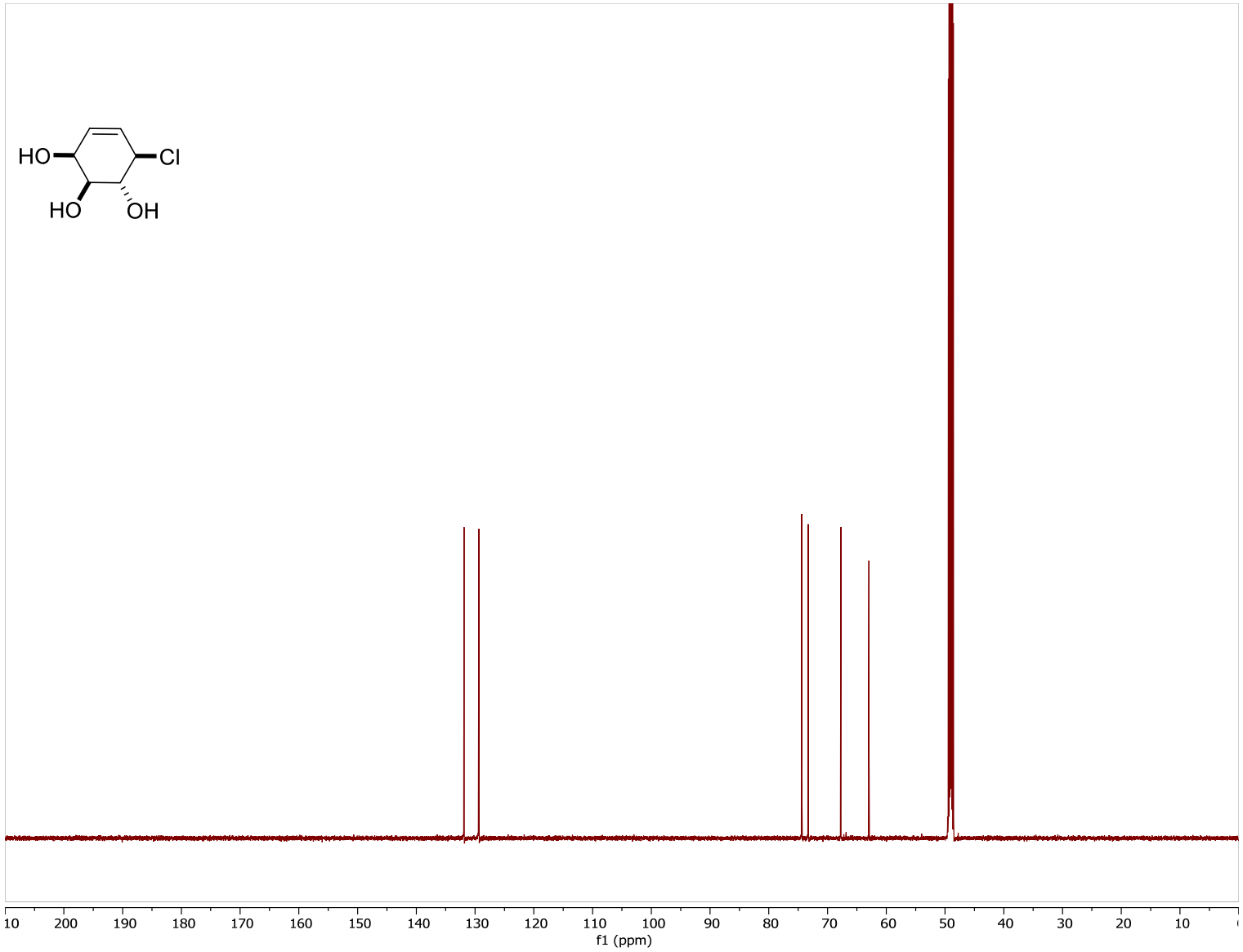


Figure S10: COSY NMR spectrum of **1** in CD_3OD.

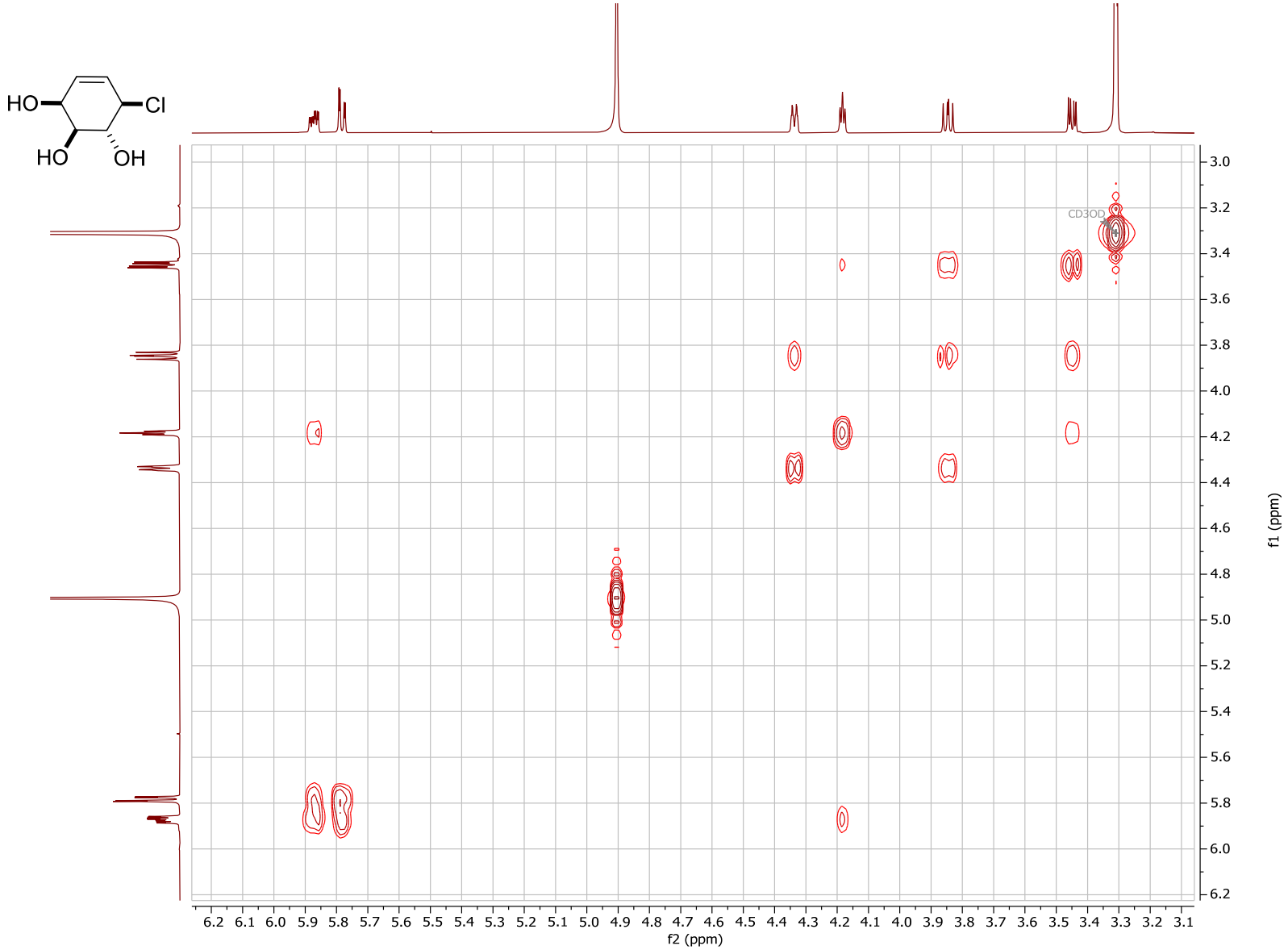


Figure S11: HSQC NMR spectrum of **1** in CD_3OD.

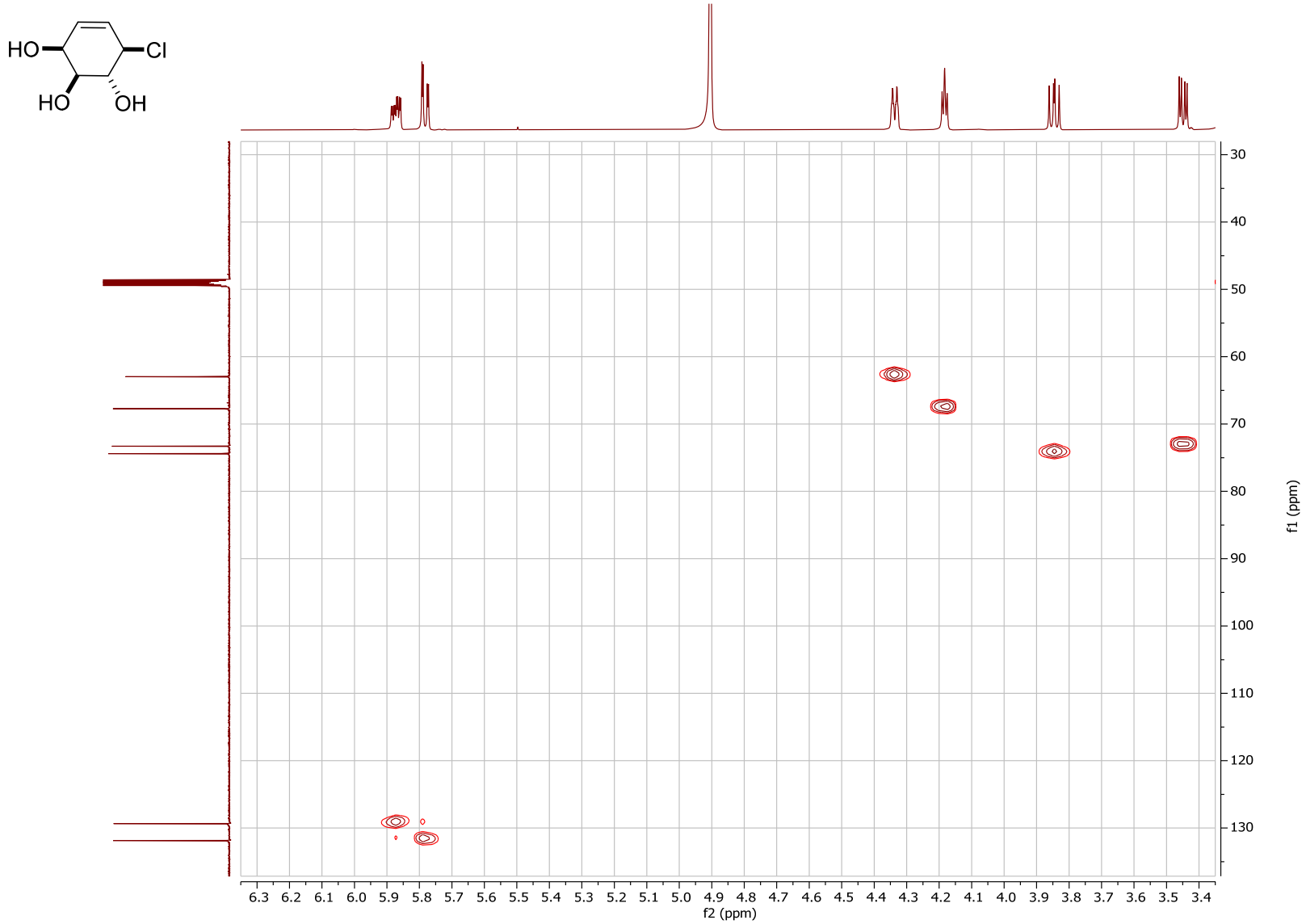


Figure S12: HMBC NMR spectrum of **1** in CD_3OD.

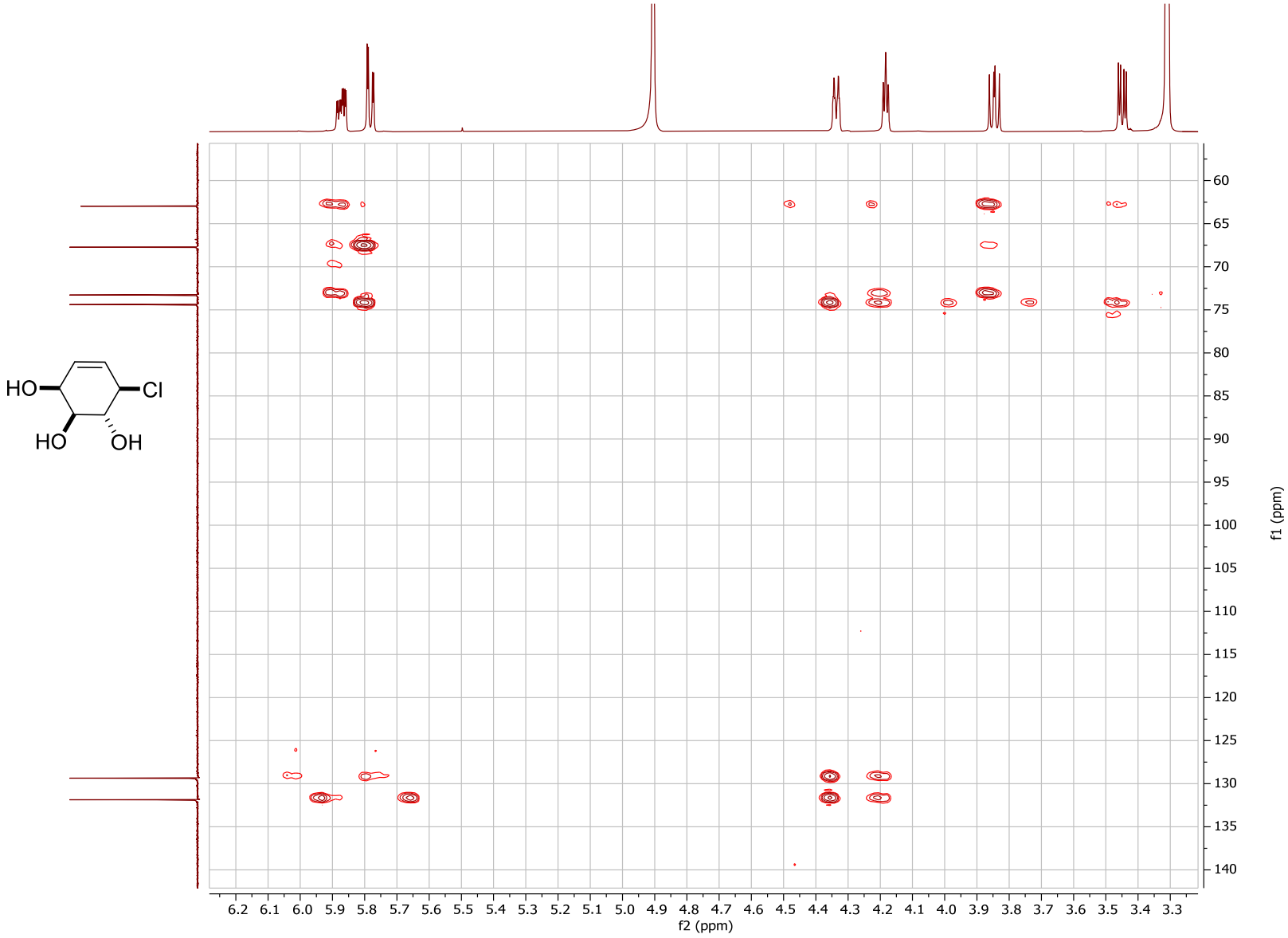


Figure S13: ^{1}H-NMR spectrum of **2** in CD_3OD (600 MHz).

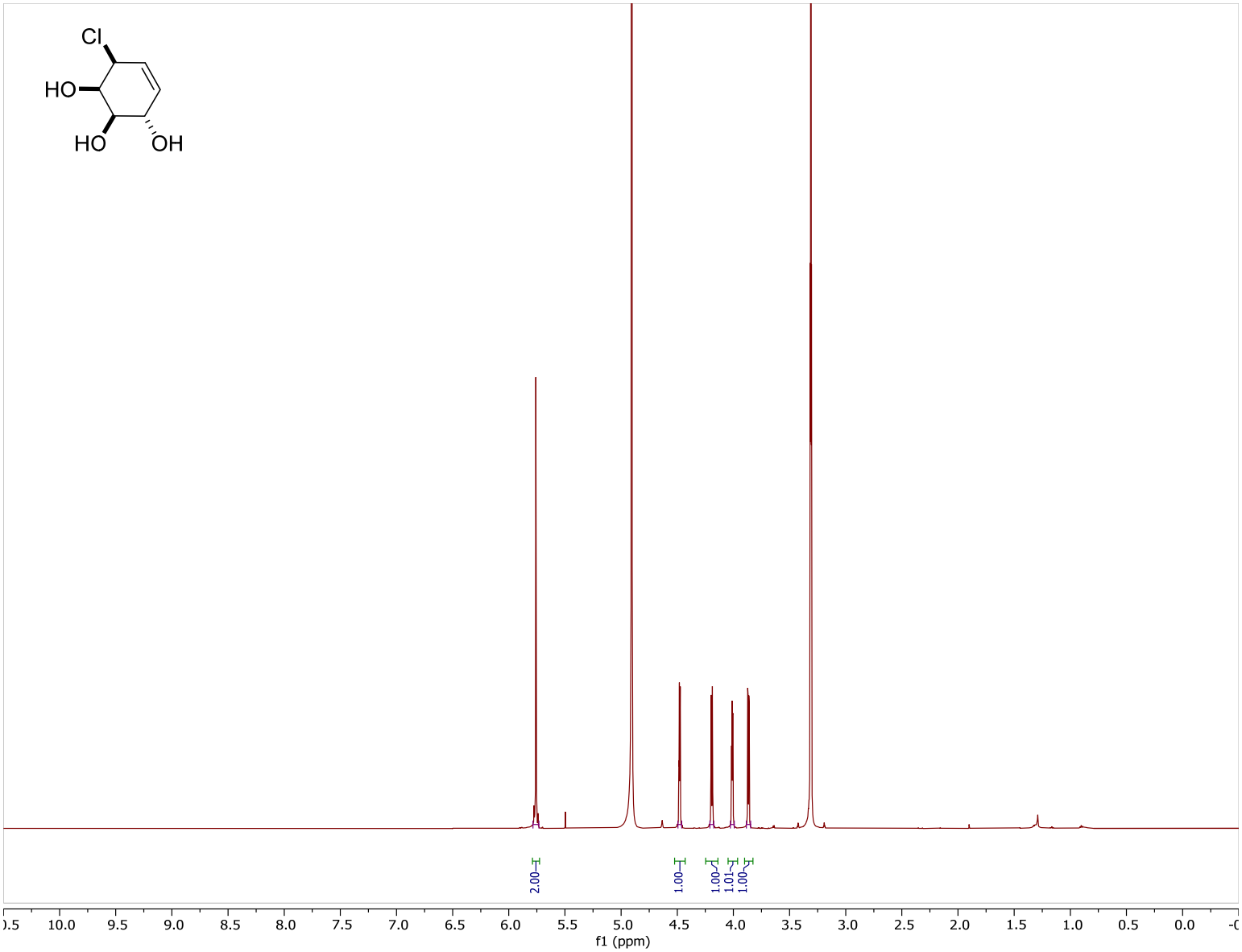


Figure S14: ^{13}C {^{1}H}-NMR spectrum of **2** in CD_3OD (151 MHz).

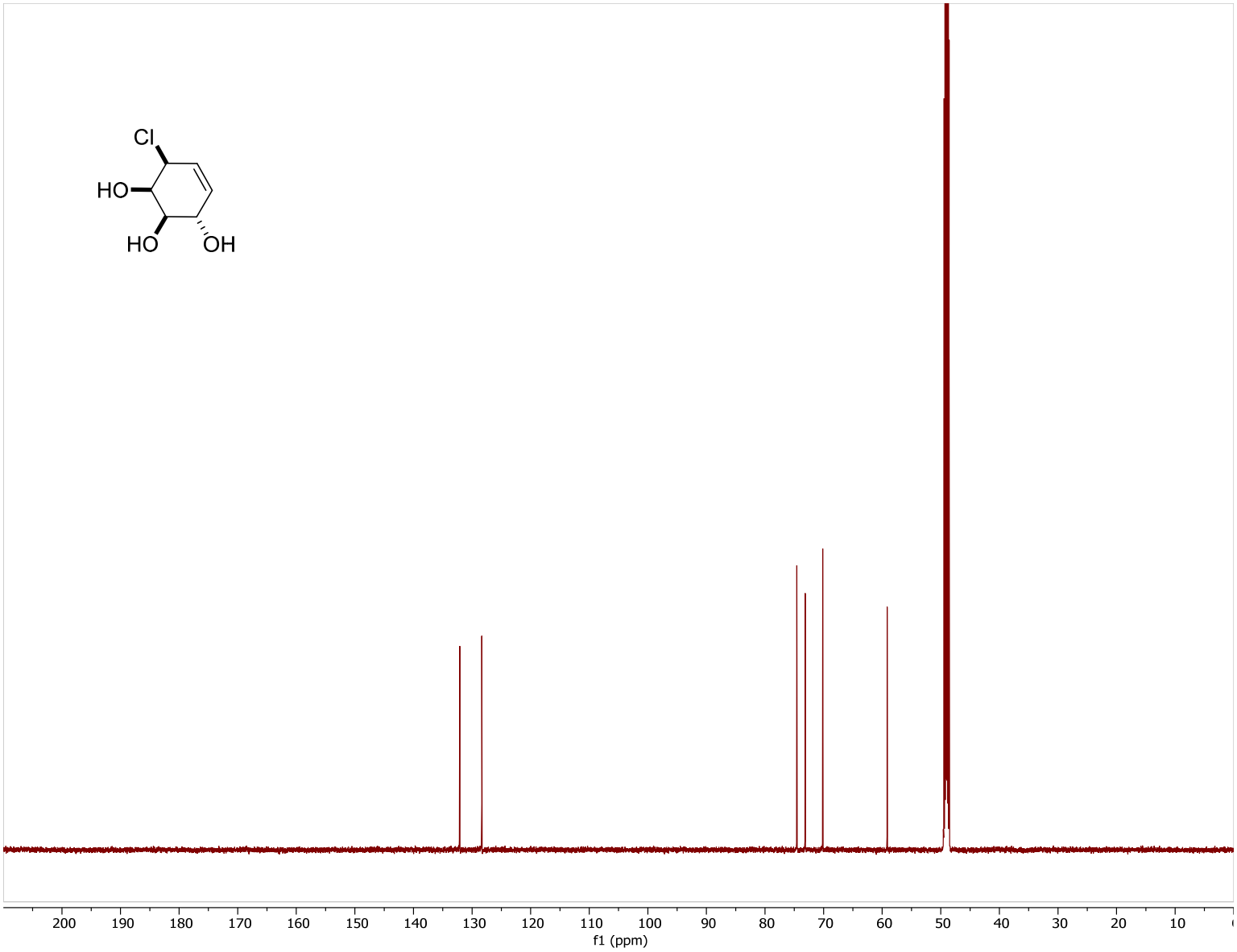


Figure S15: COSY NMR spectrum of **2** in CD_3OD.

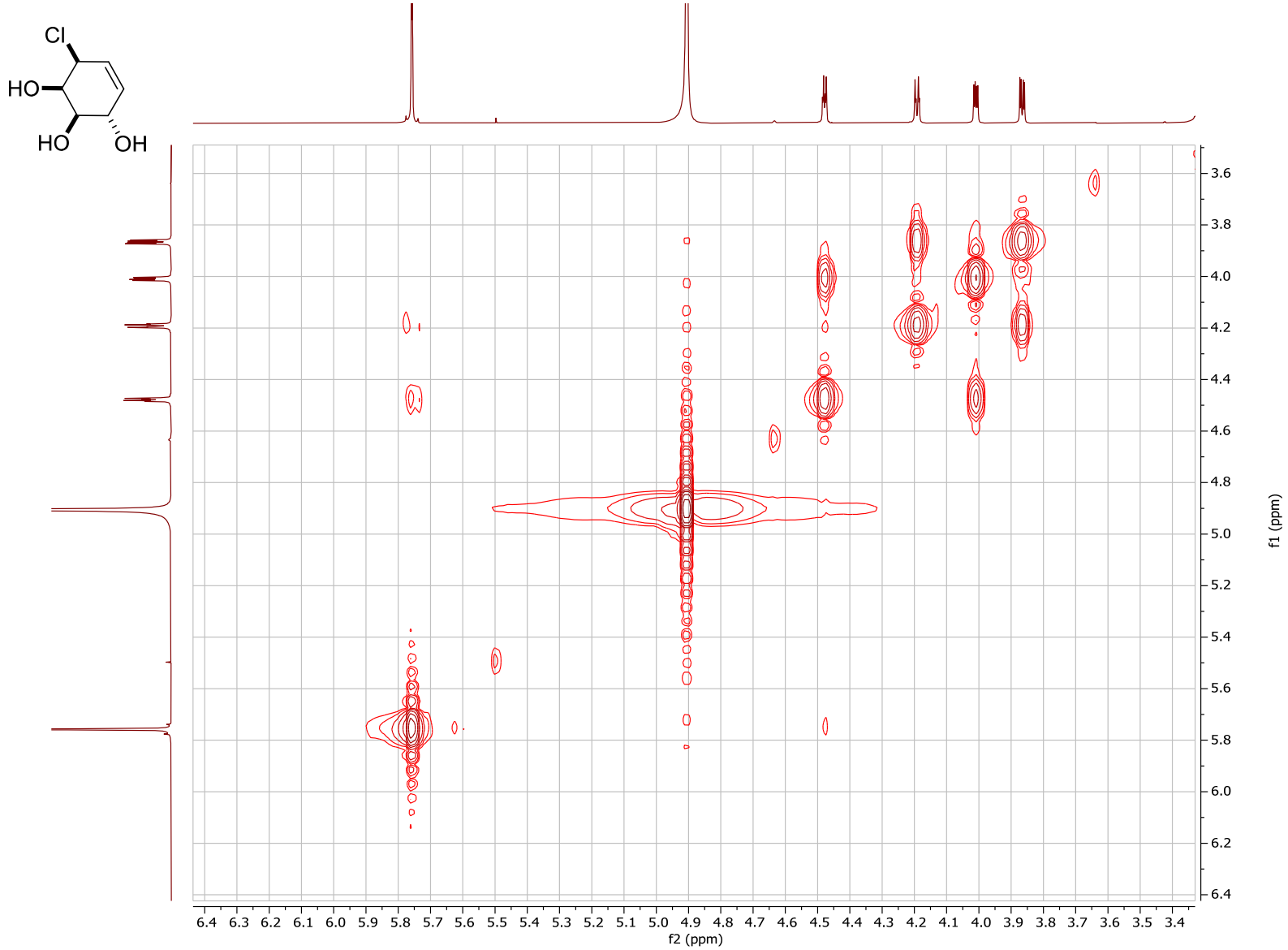


Figure S16: HSQC NMR spectrum of **2** in CD_3OD.

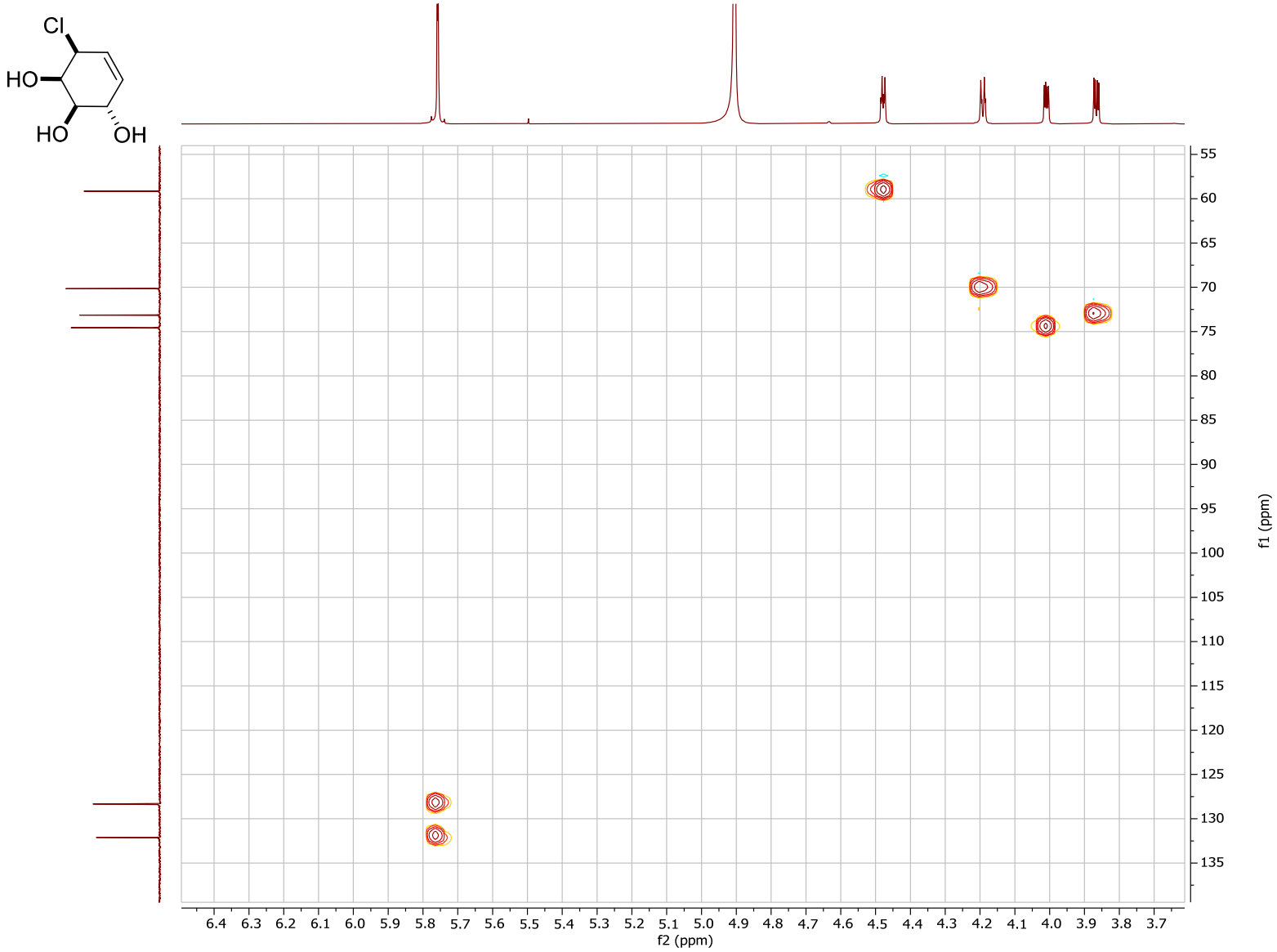


Figure S17: HMBC NMR spectrum of **2** in CD_3OD.

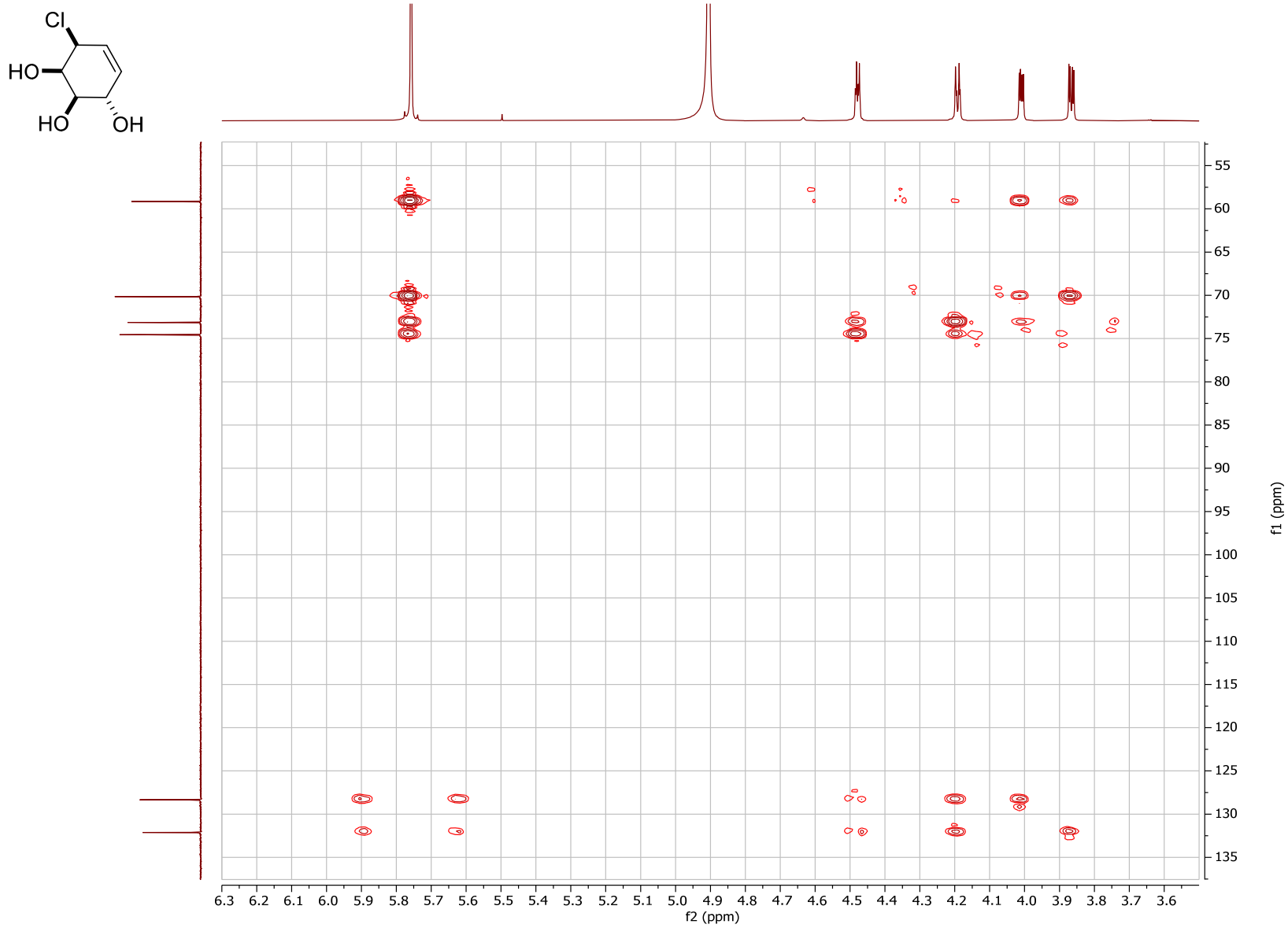


Figure S18: ^{1}H-NMR spectrum of **3** in CD_3OD (600 MHz).

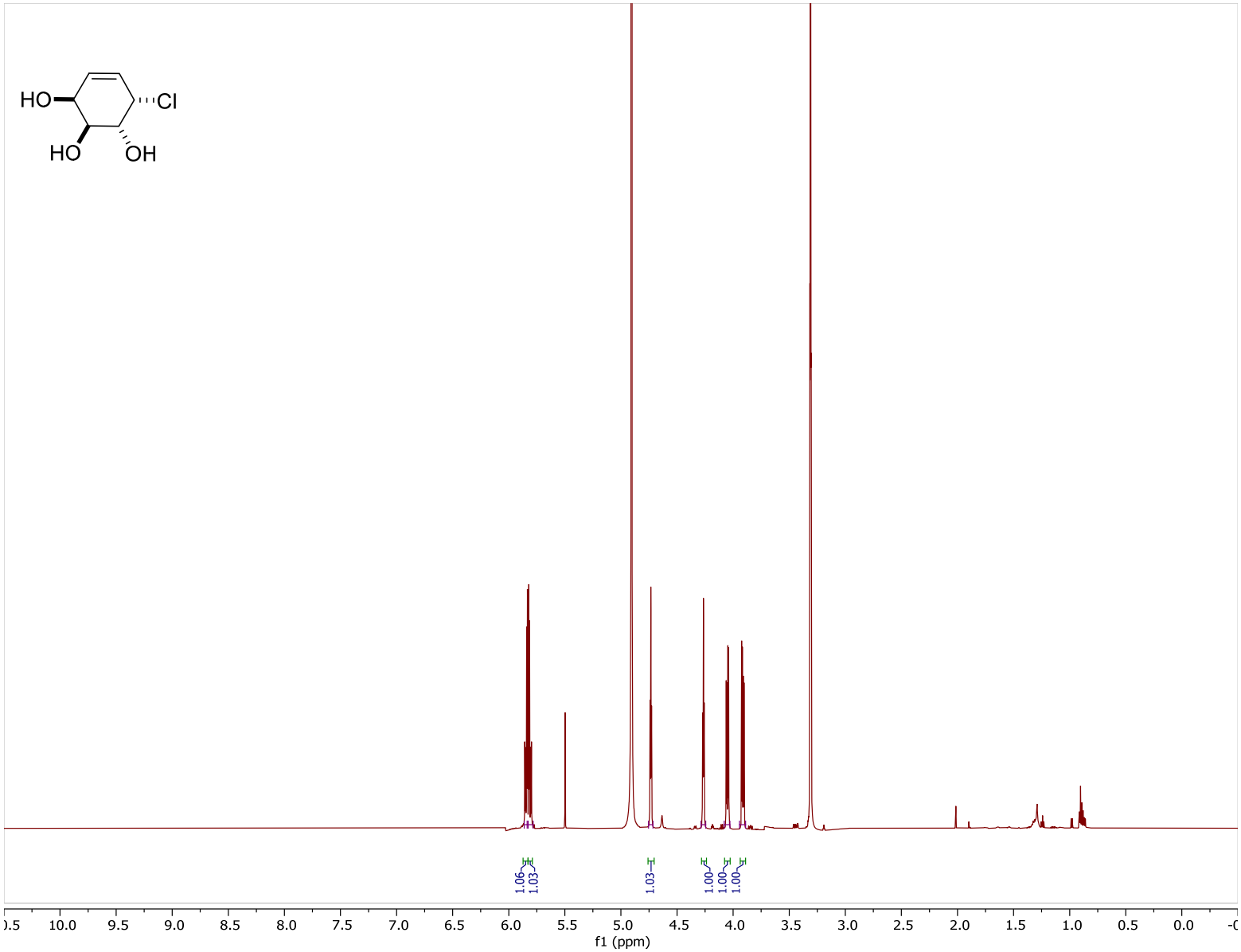


Figure S19: ^{13}C {^{1}H}-NMR spectrum of **3** in CD_3OD (151 MHz).

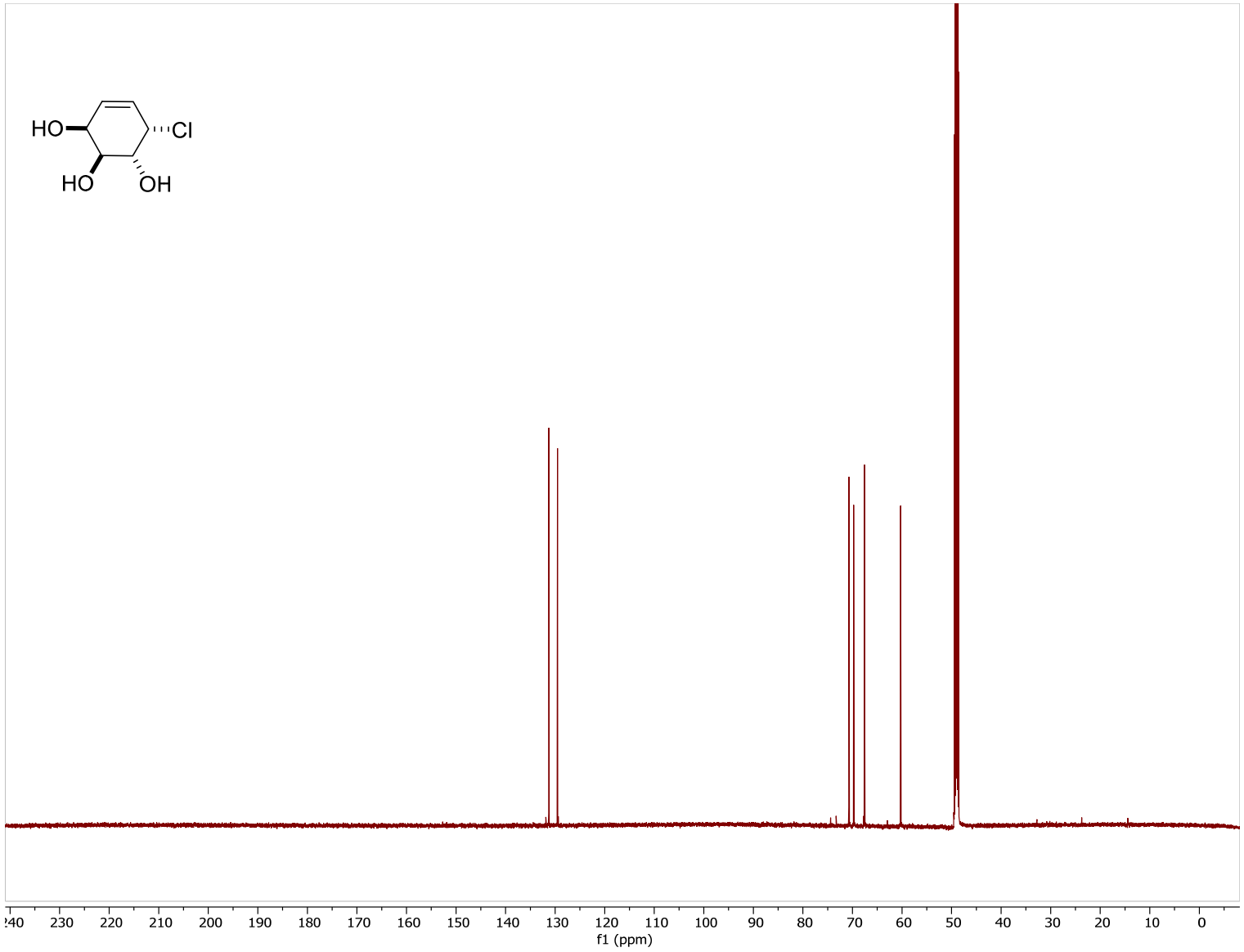


Figure S20: COSY NMR spectrum of **3** in CD_3OD.

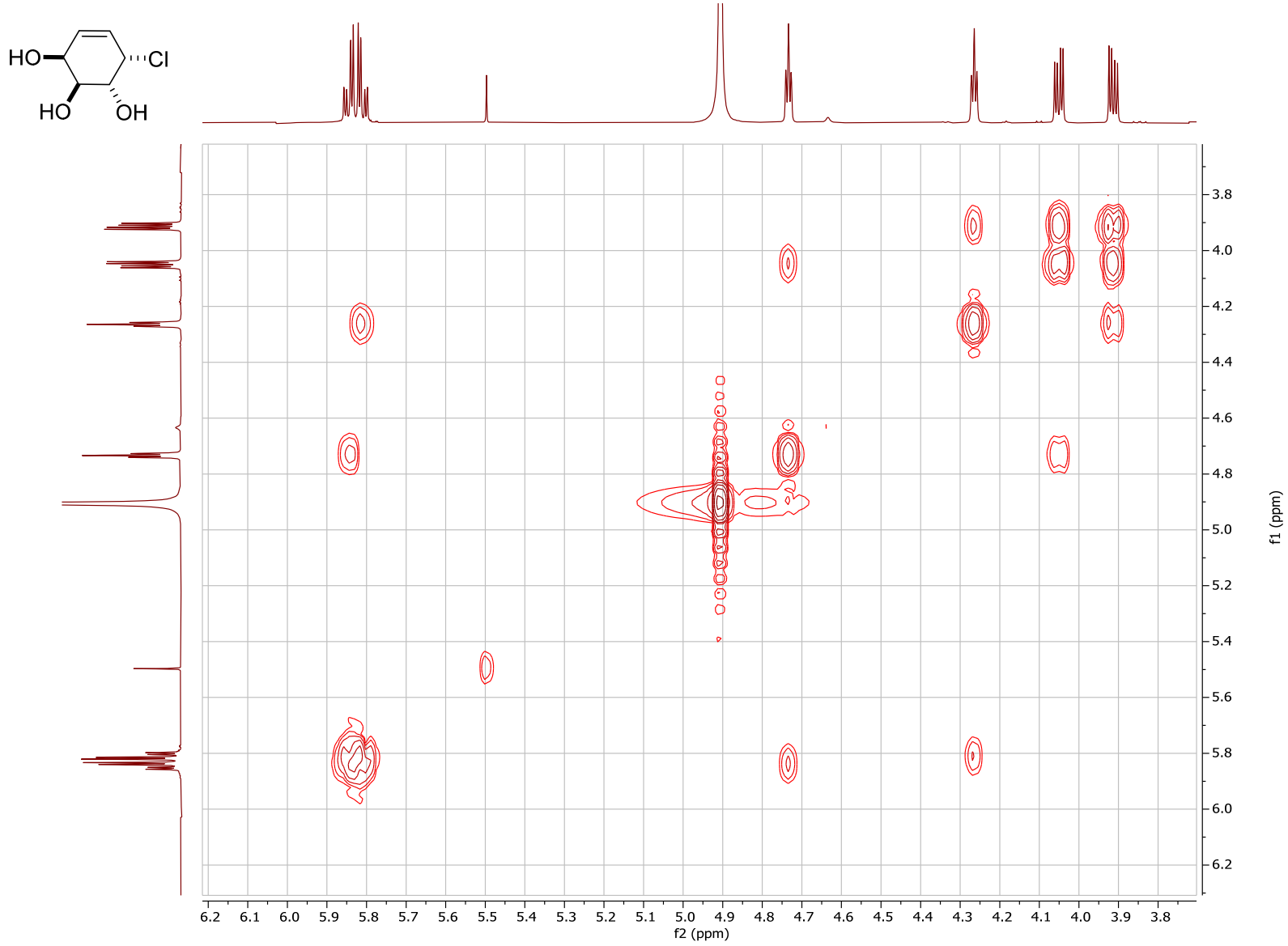


Figure S21: HSQC NMR spectrum of **3** in CD_3OD.

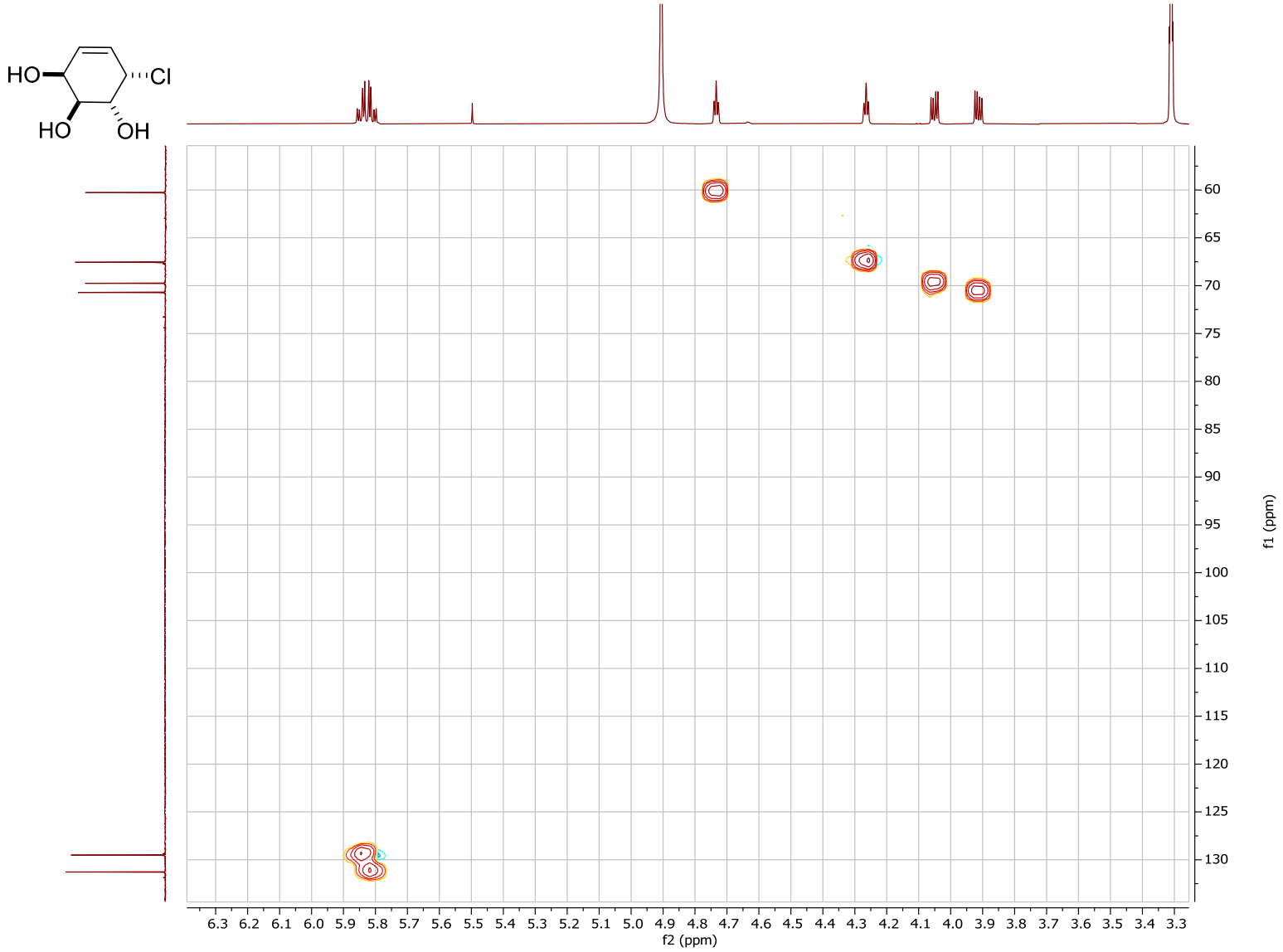


Figure S22: HMBC NMR spectrum of **3** in CD_3OD.

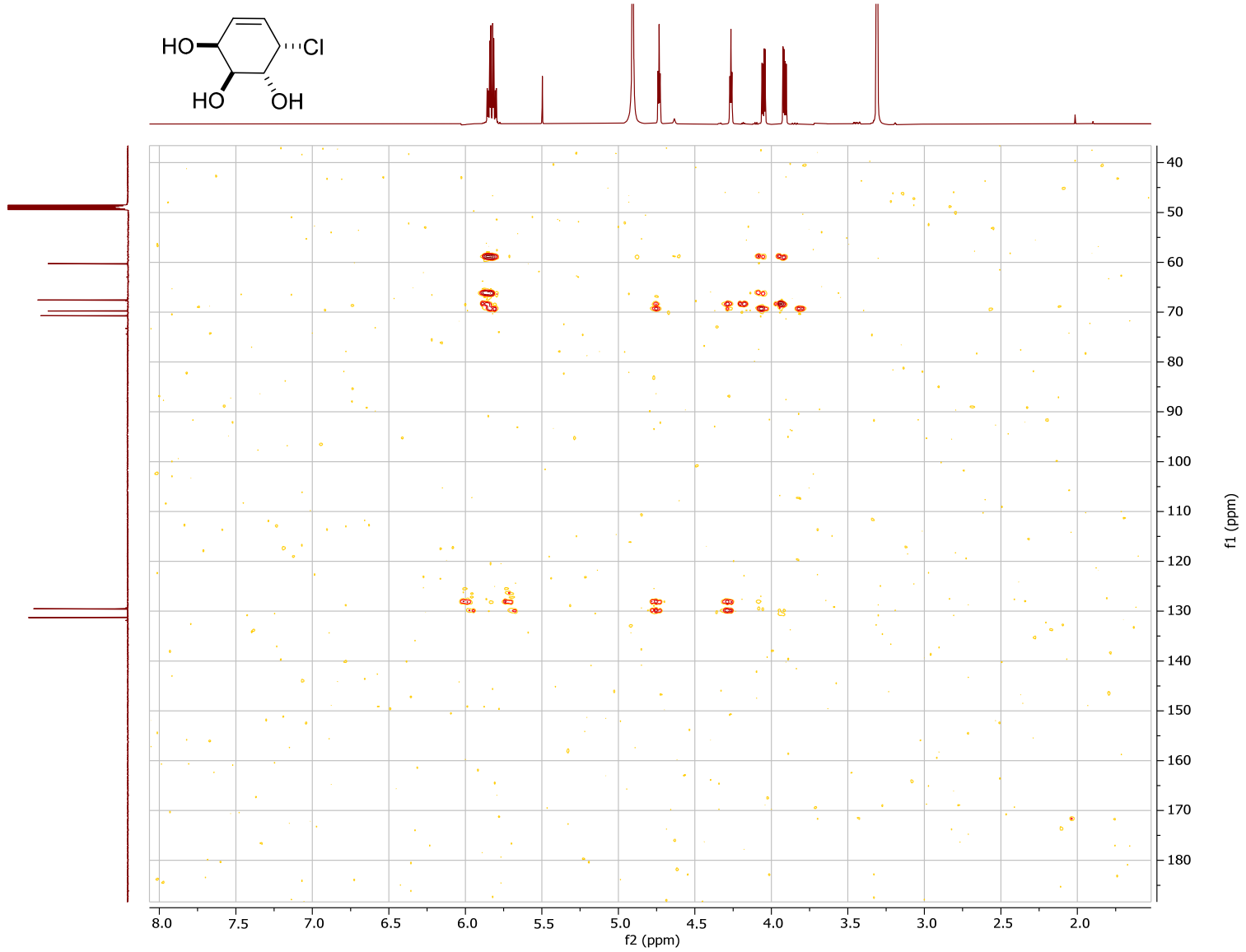


Figure S23: ^{1}H-NMR spectrum of **4** in CD_3OD (600 MHz).

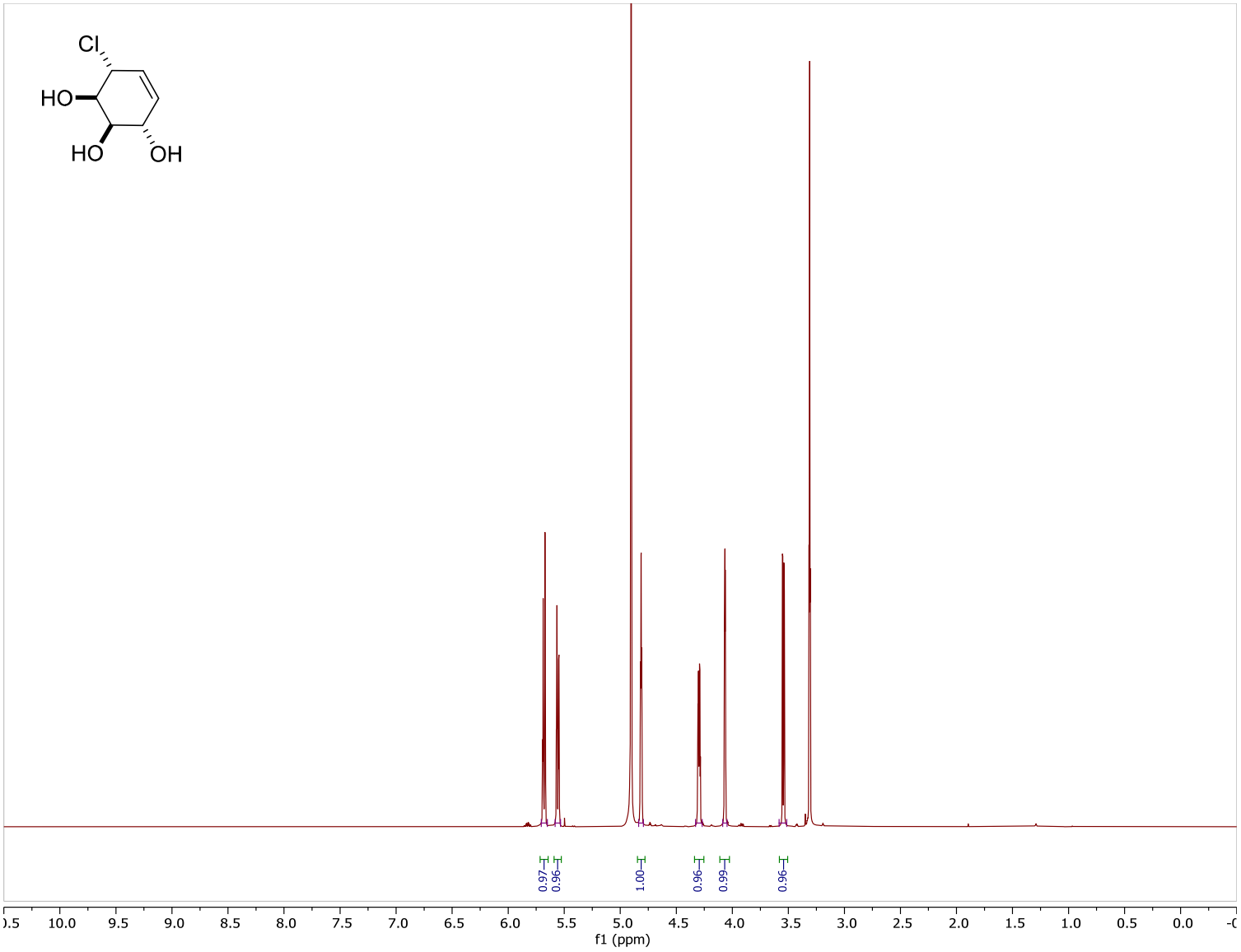


Figure S24: ^{13}C {^{1}H}-NMR spectrum of **4** in CD_3OD (151 MHz).

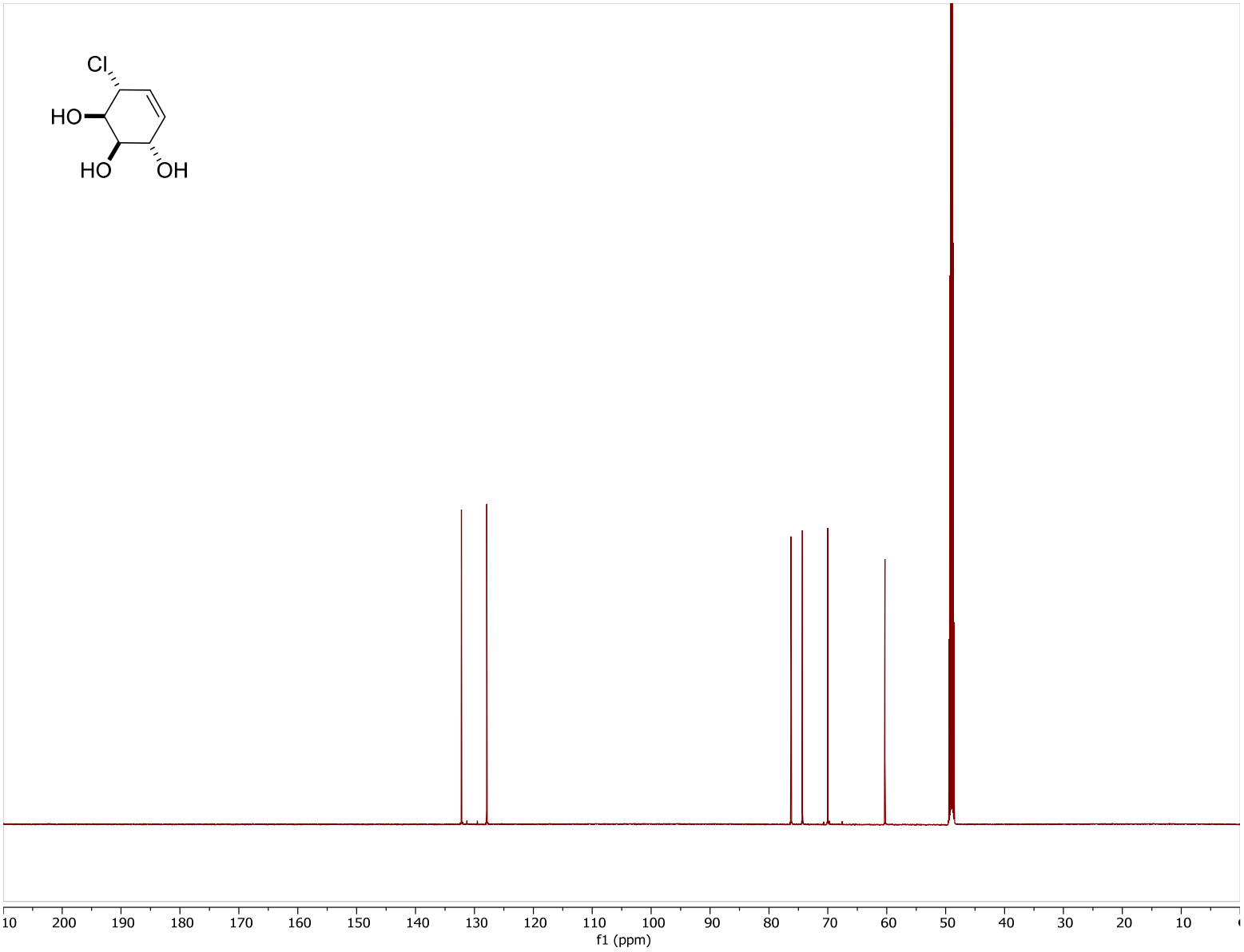


Figure S25: COSY NMR spectrum of **4** in CD_3OD.

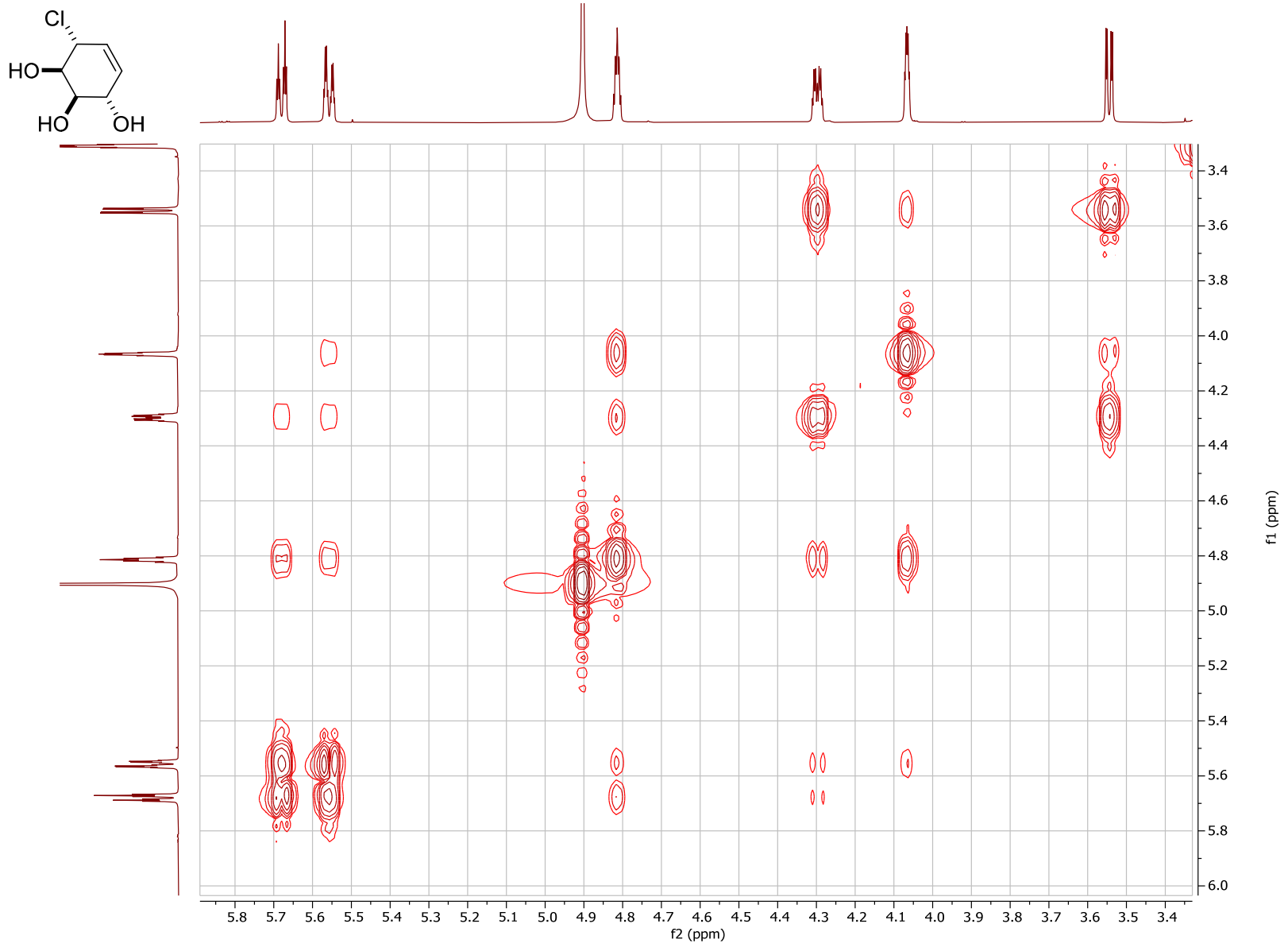


Figure S26: HSQC NMR spectrum of **4** in CD_3OD

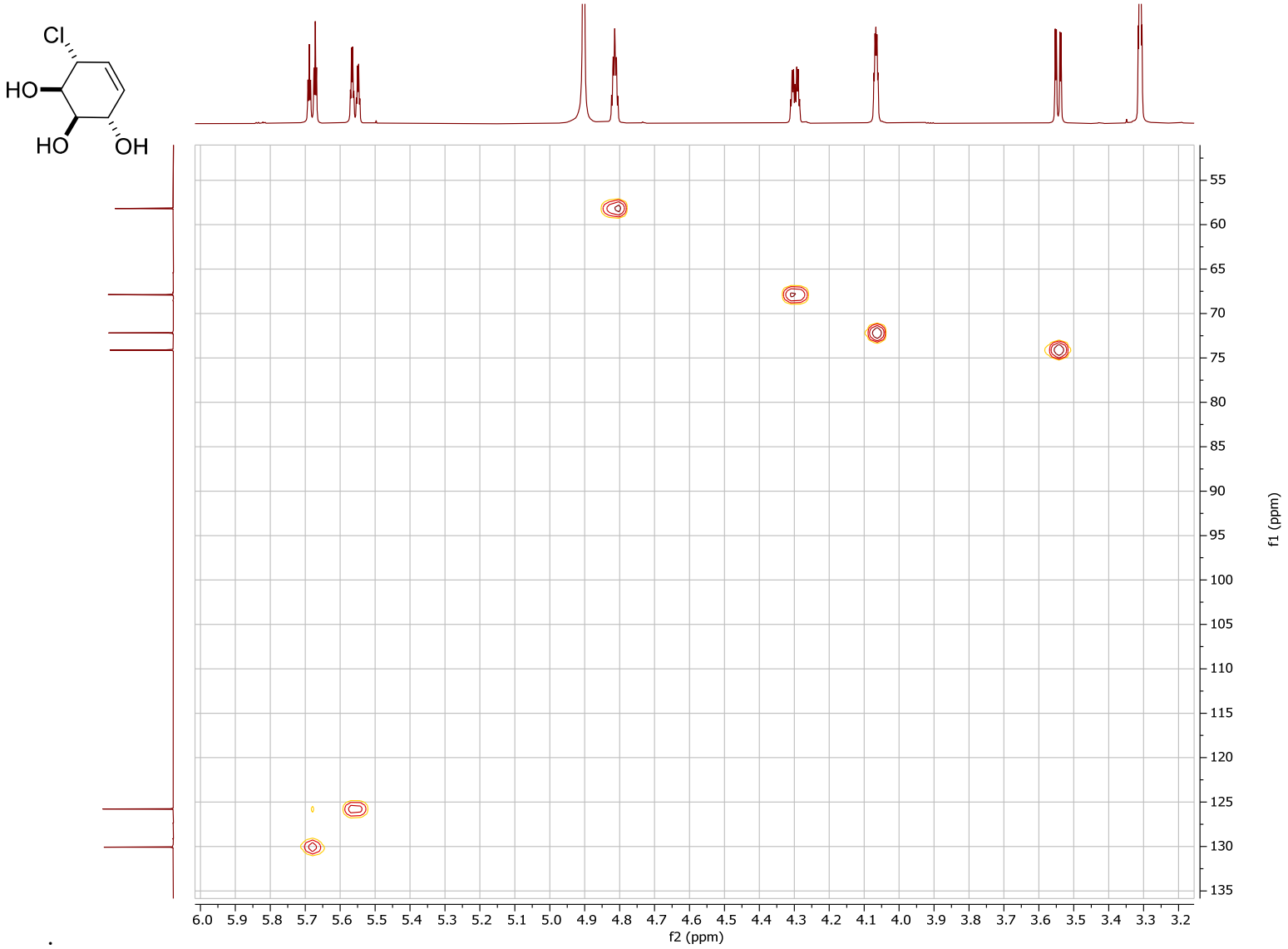


Figure S27: HMBC NMR spectrum of **4** in CD_3OD.

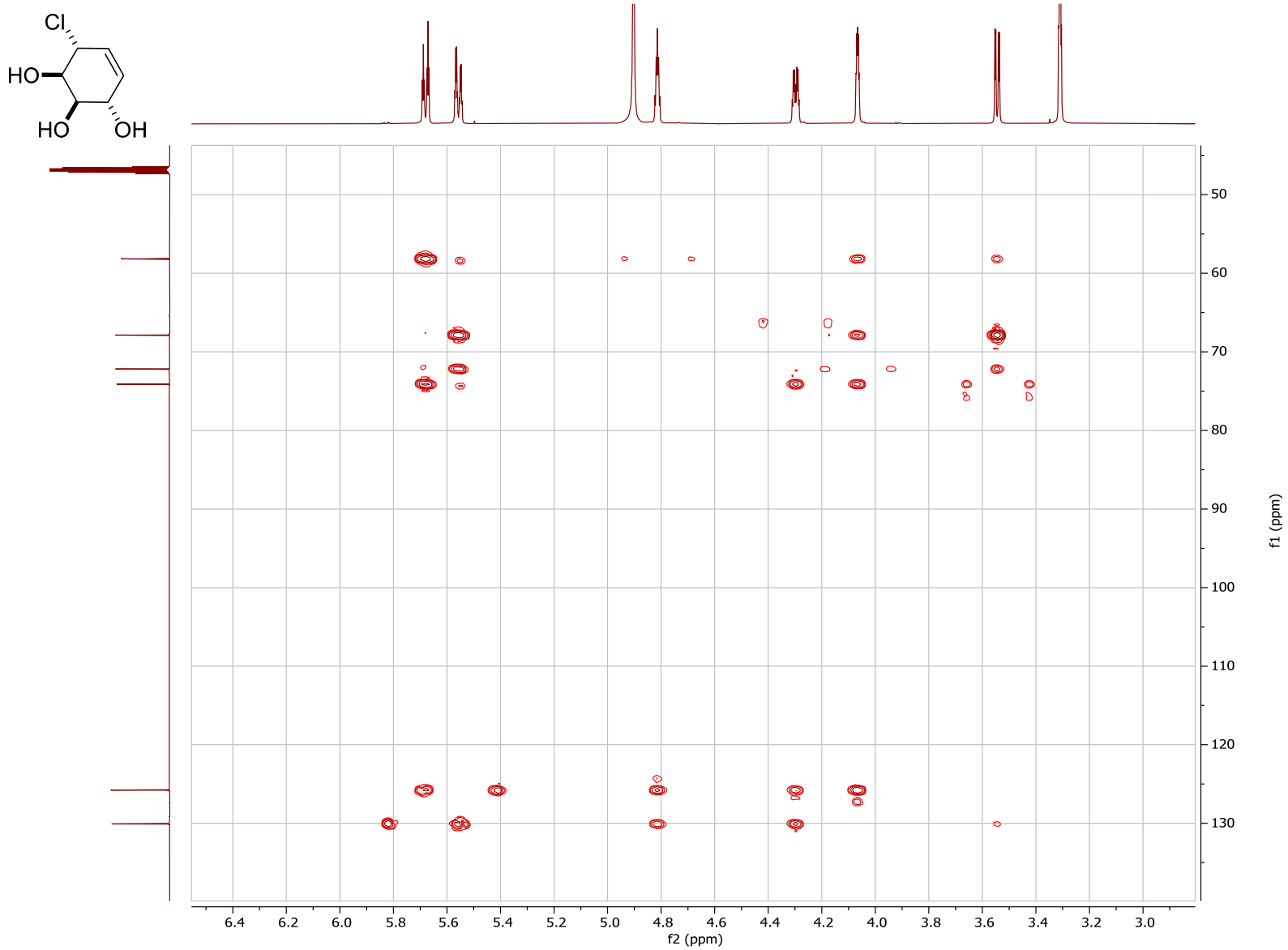


Figure S28: ^{1}H-NMR spectrum of **6** in $CDCl_3$ (600 MHz).

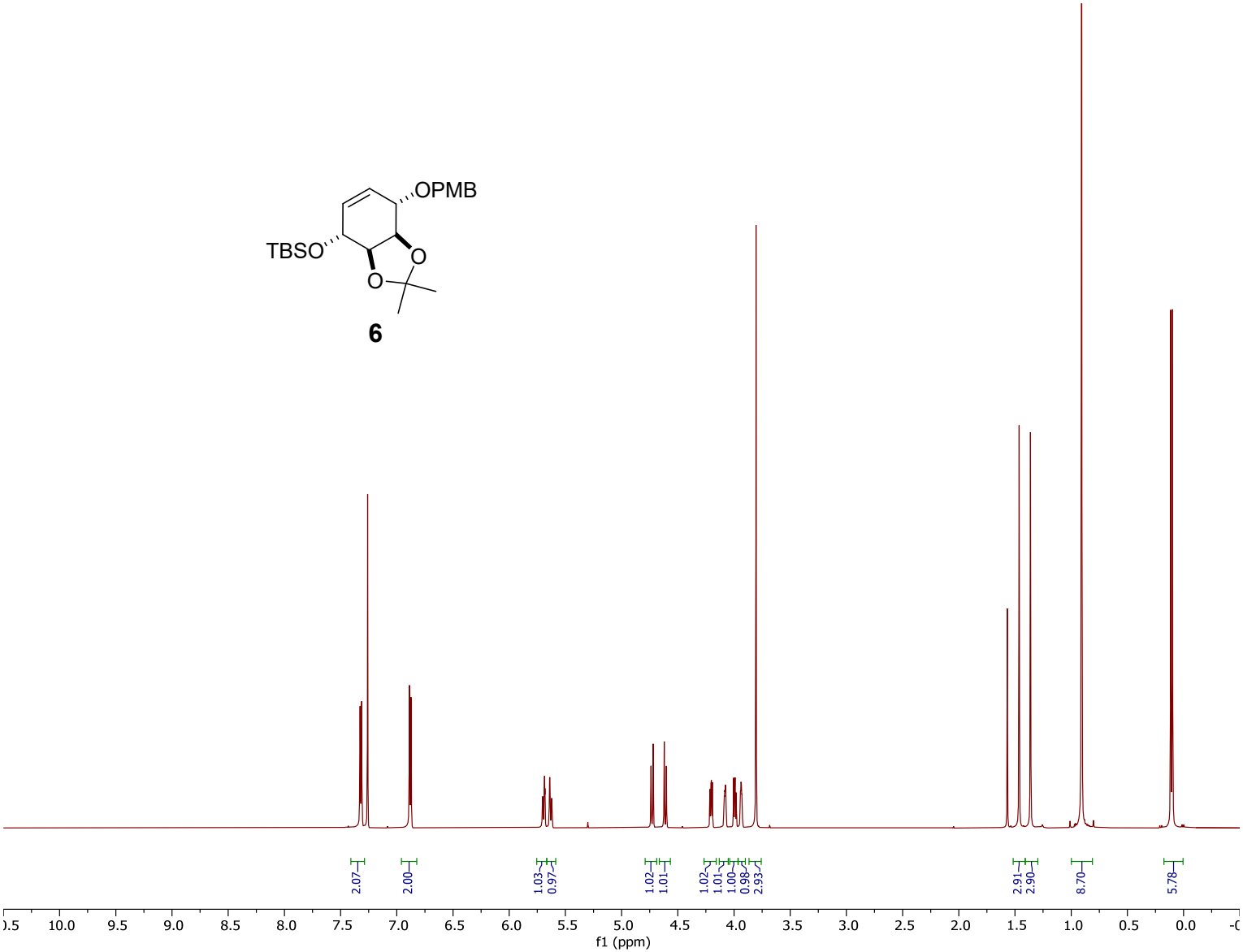


Figure S29: ^{13}C {^{1}H}-NMR spectrum of **6** in $CDCl_3$ (151 MHz).

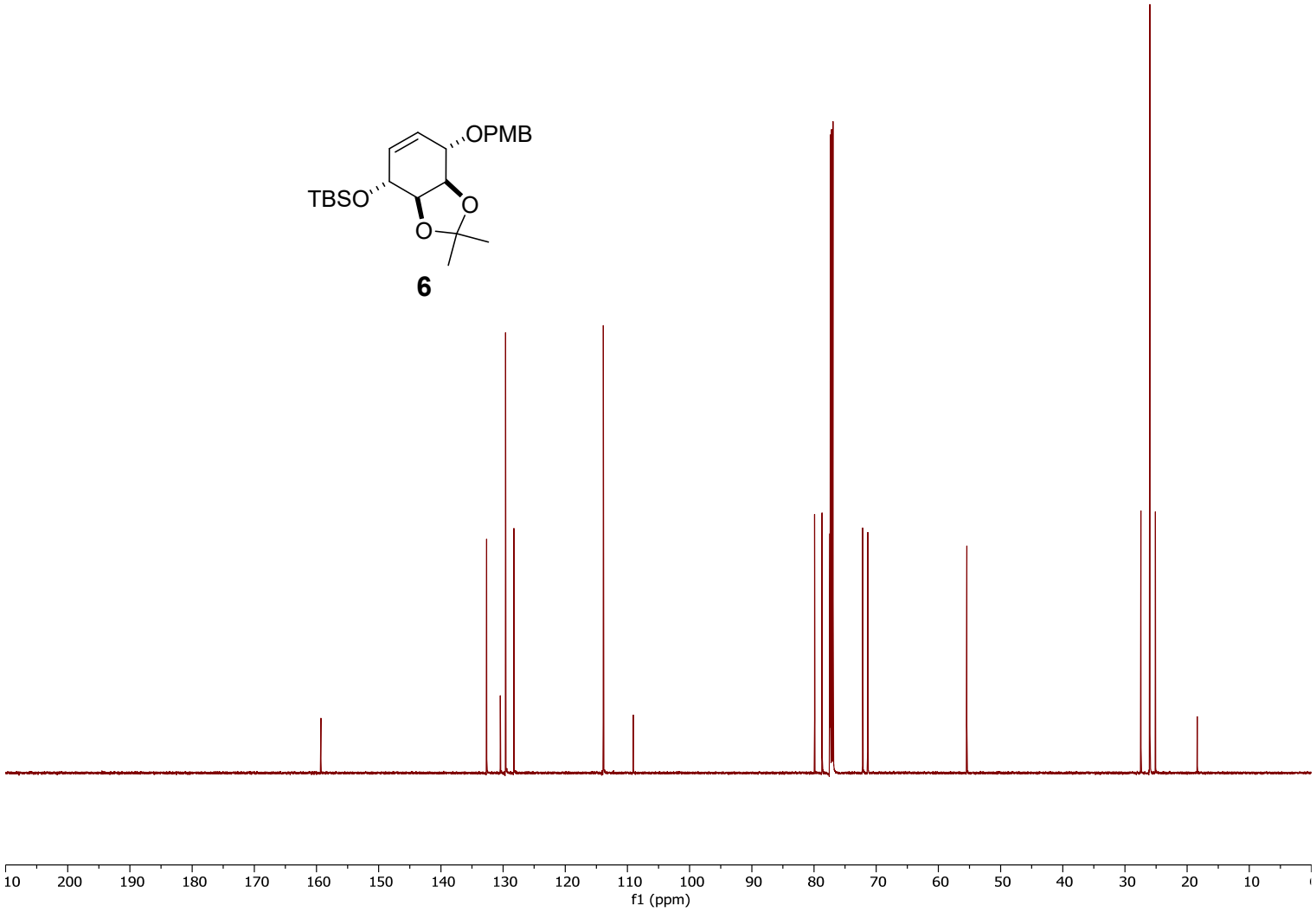


Figure S30: ^{1}H-NMR spectrum of **7** in $CDCl_3$ (600 MHz).

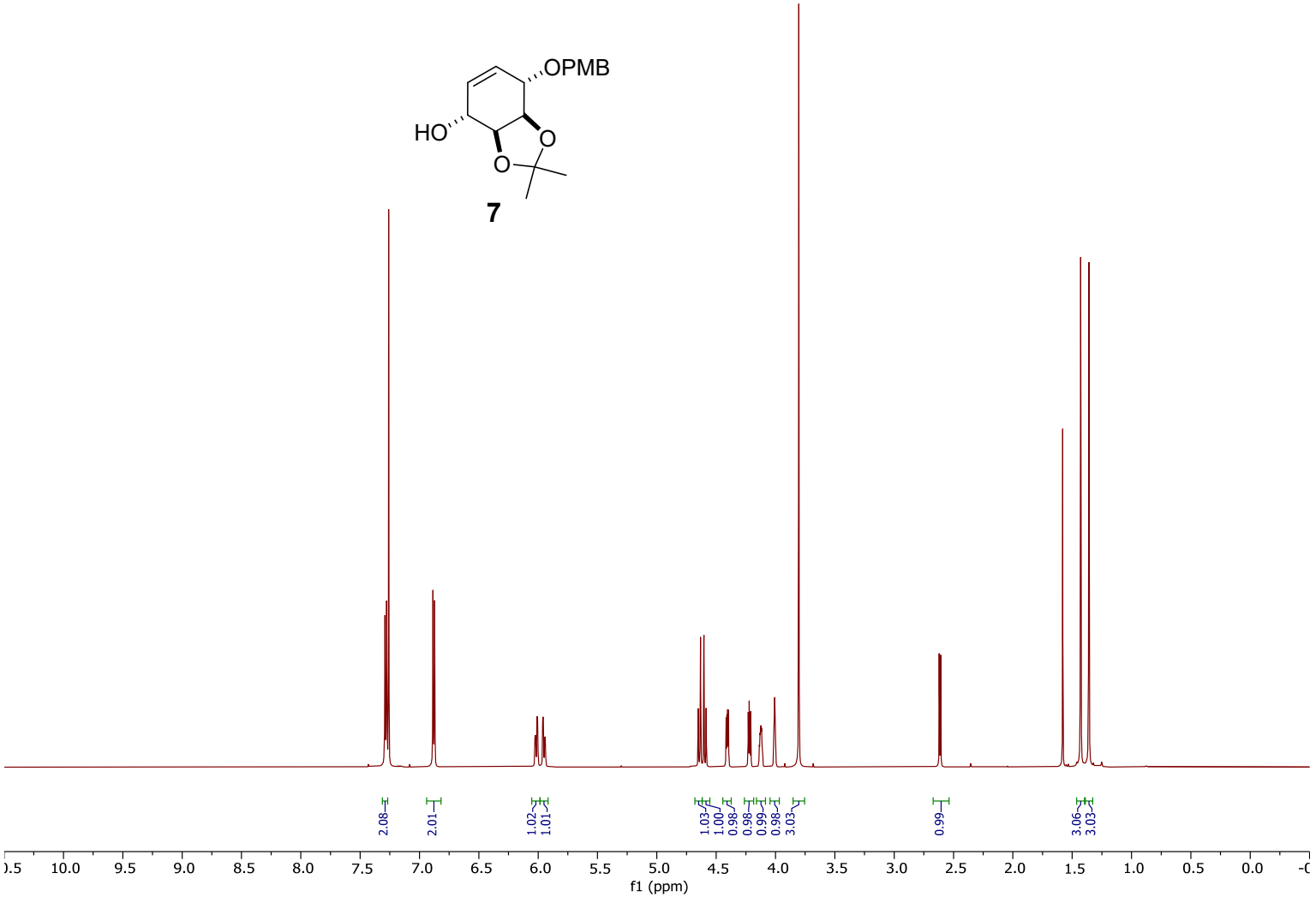


Figure S31: ^{13}C $\{^{1}H\}$-NMR spectrum of **7** in $CDCl_3$ (151 MHz).

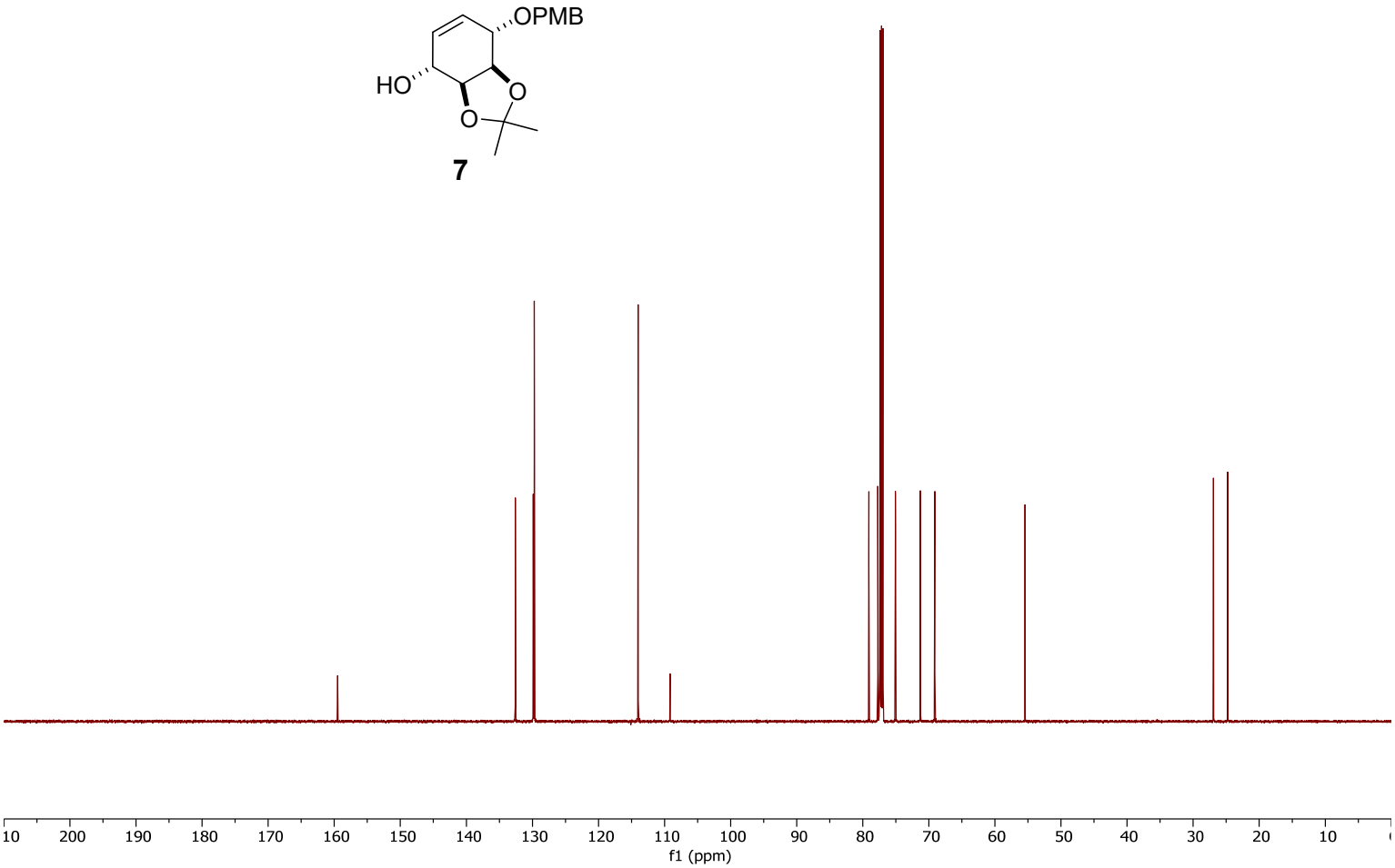


Figure S32: ^{1}H-NMR spectrum of **8** in $CDCl_3$ (600 MHz).

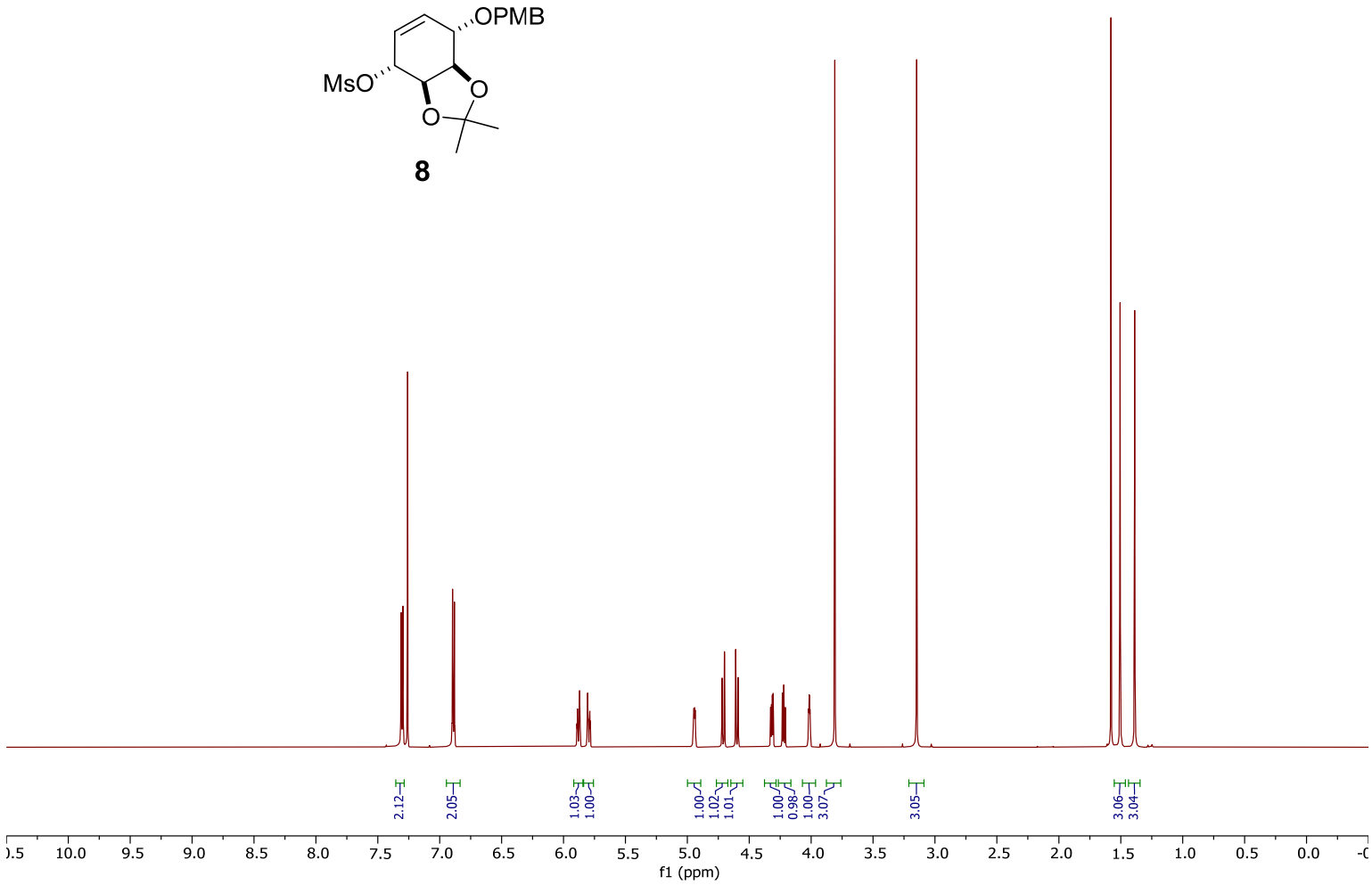


Figure S33: ^{13}C $\{^{1}H\}$-NMR spectrum of **8** in $CDCl_3$ (151 MHz).

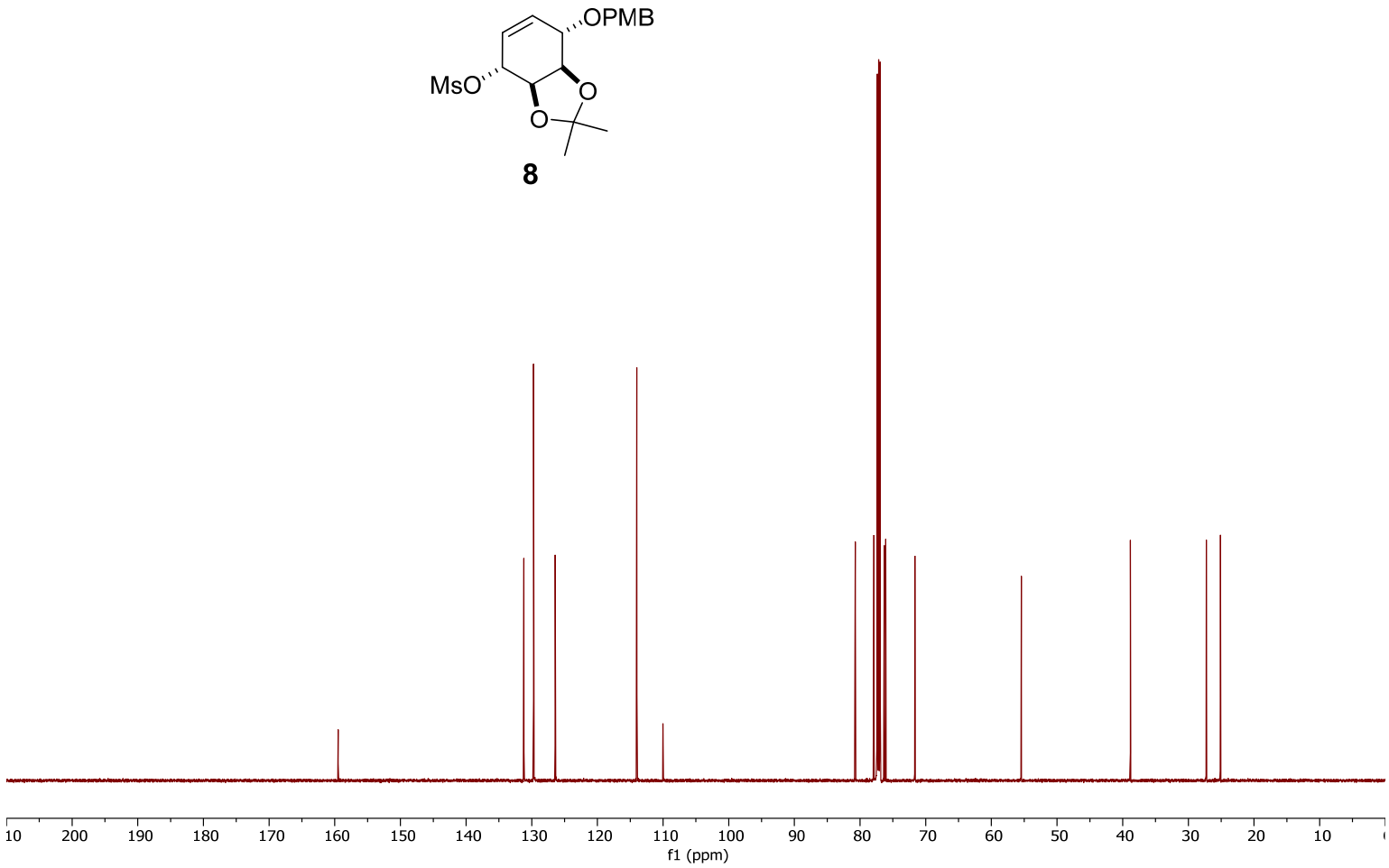


Figure S34: ^{1}H-NMR spectrum of **9a** in $CDCl_3$ (600 MHz).

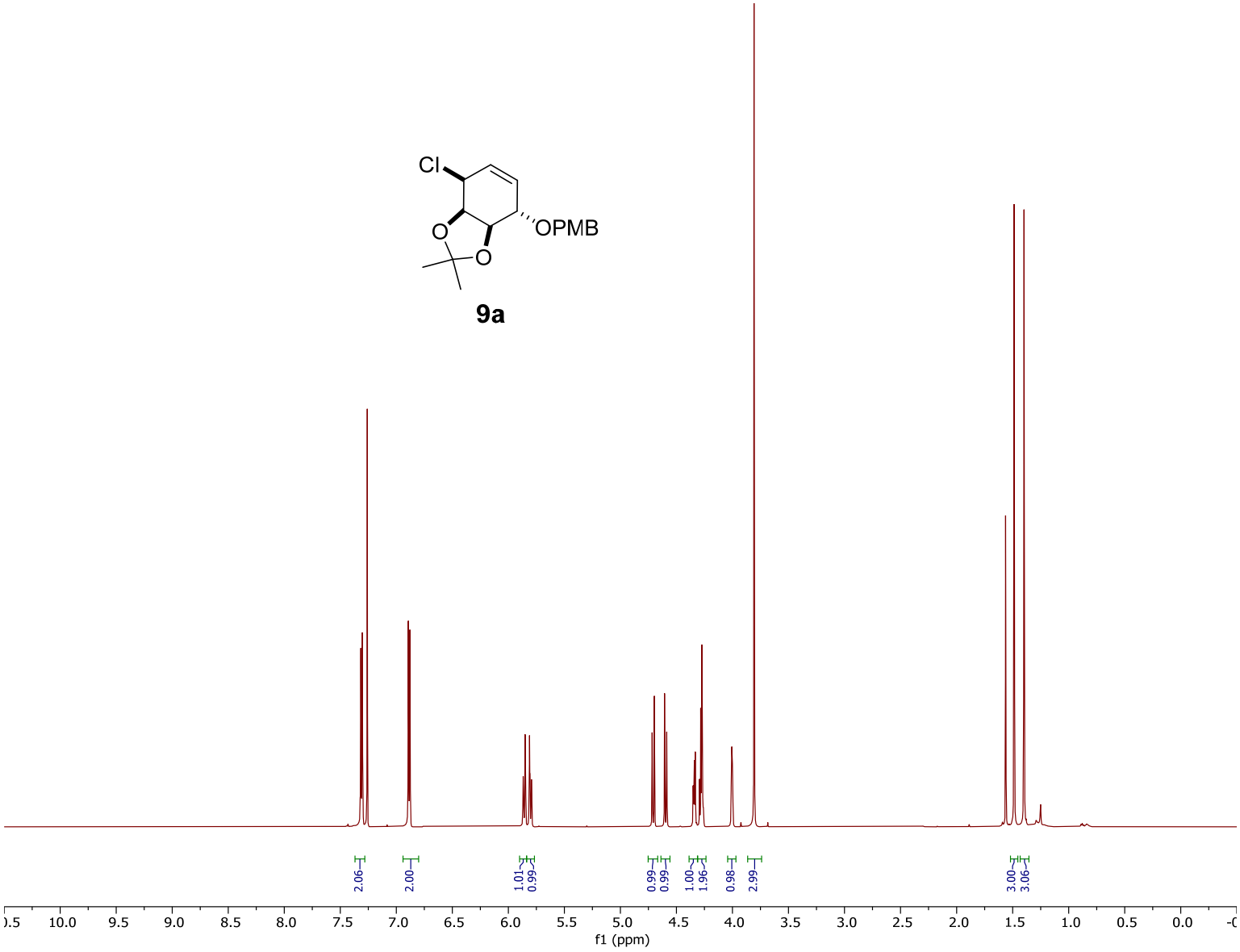


Figure S35: ^{13}C $\{^{1}H\}$-NMR spectrum of **9a** in $CDCl_3$ (151 MHz).

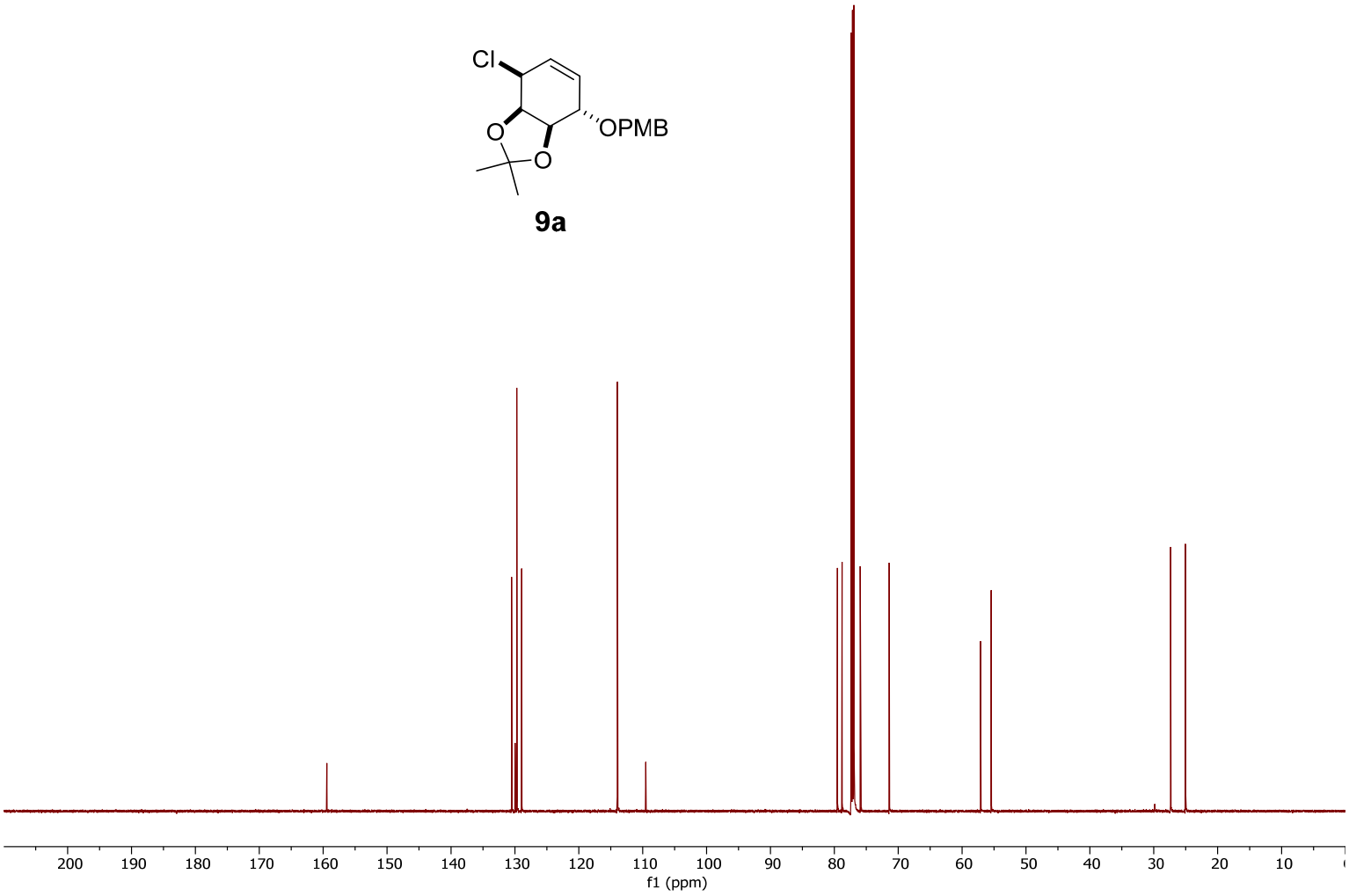


Figure S36: COSY NMR spectrum of **9a** in $CDCl_3$.

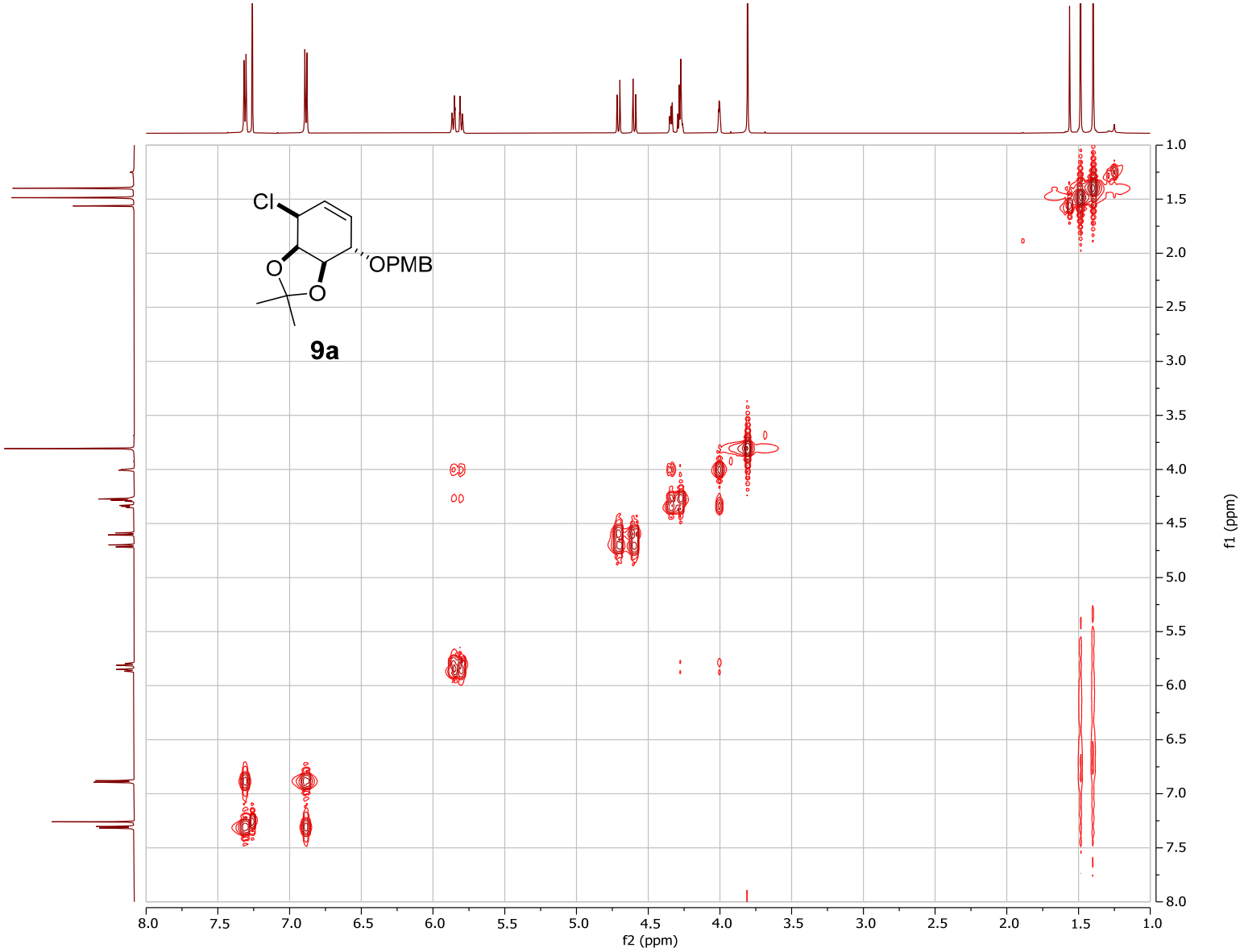


Figure S37: HSQC NMR spectrum of **9a** in $CDCl_3$.

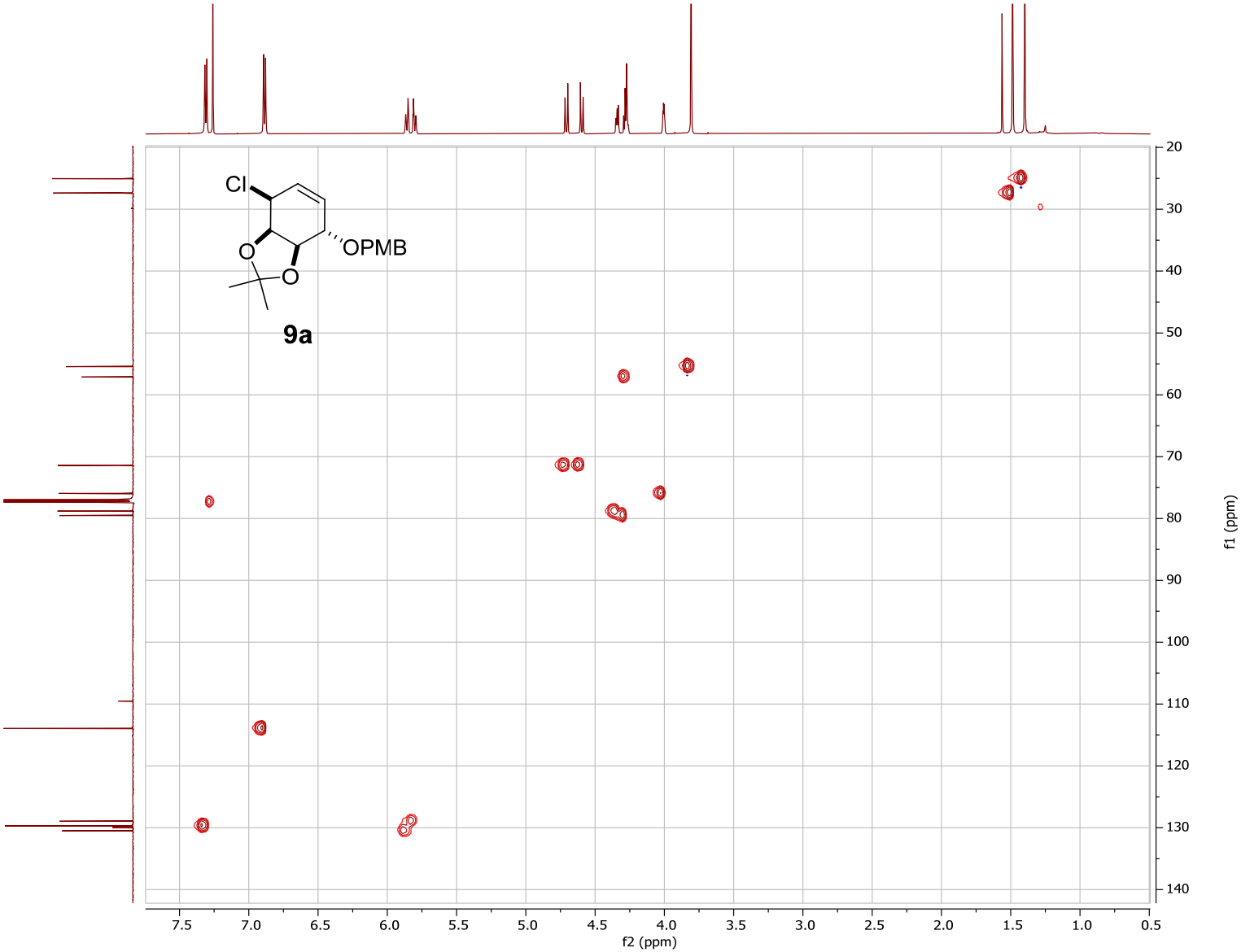


Figure S38: ^{1}H-NMR spectrum of **9c** in $CDCl_3$ (600 MHz).

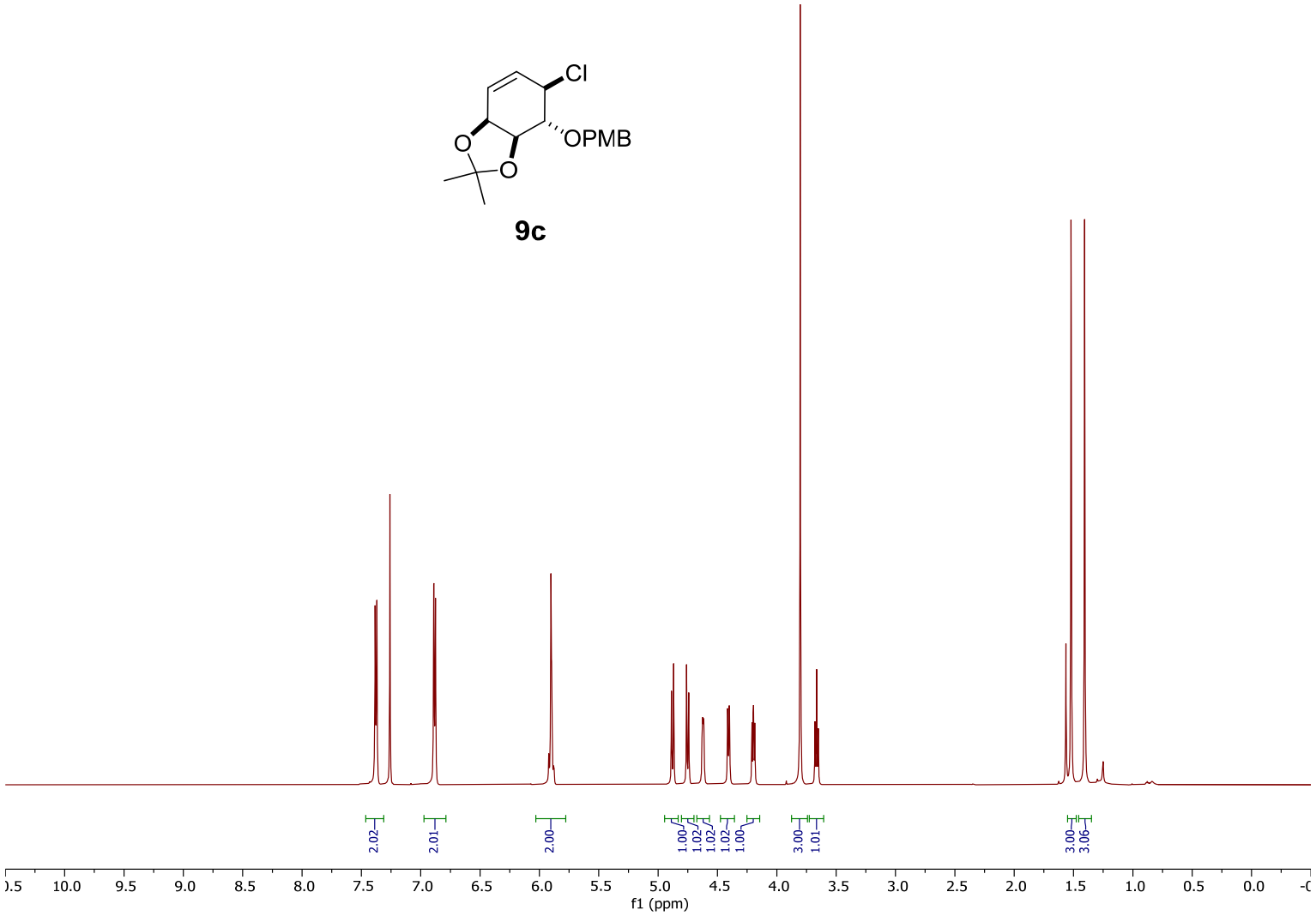


Figure S39: ^{13}C $\{^{1}H\}$-NMR spectrum of **9c** in $CDCl_3$ (151 MHz).

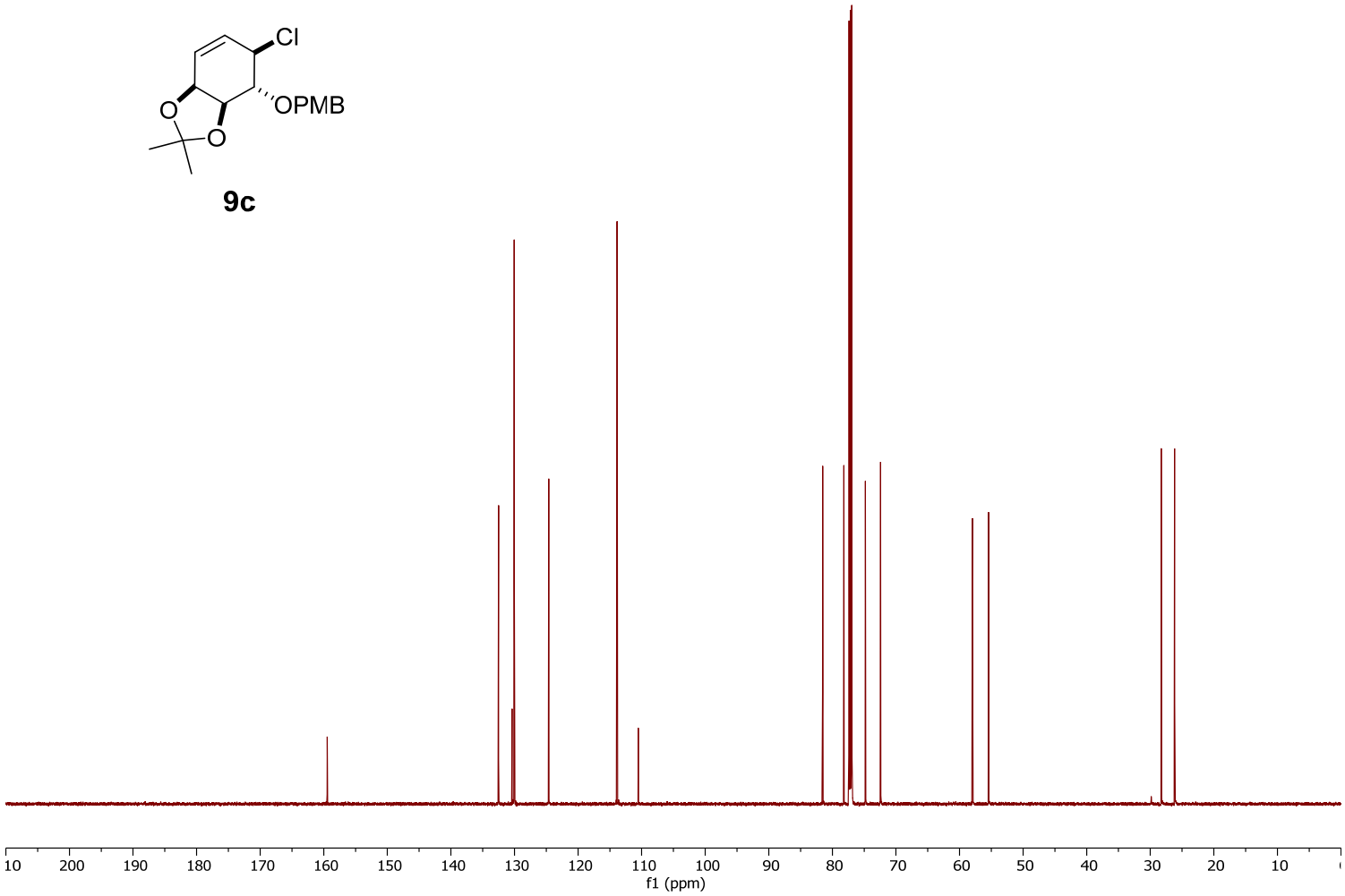


Figure S40: COSY NMR spectrum of **9c** in $CDCl_3$.

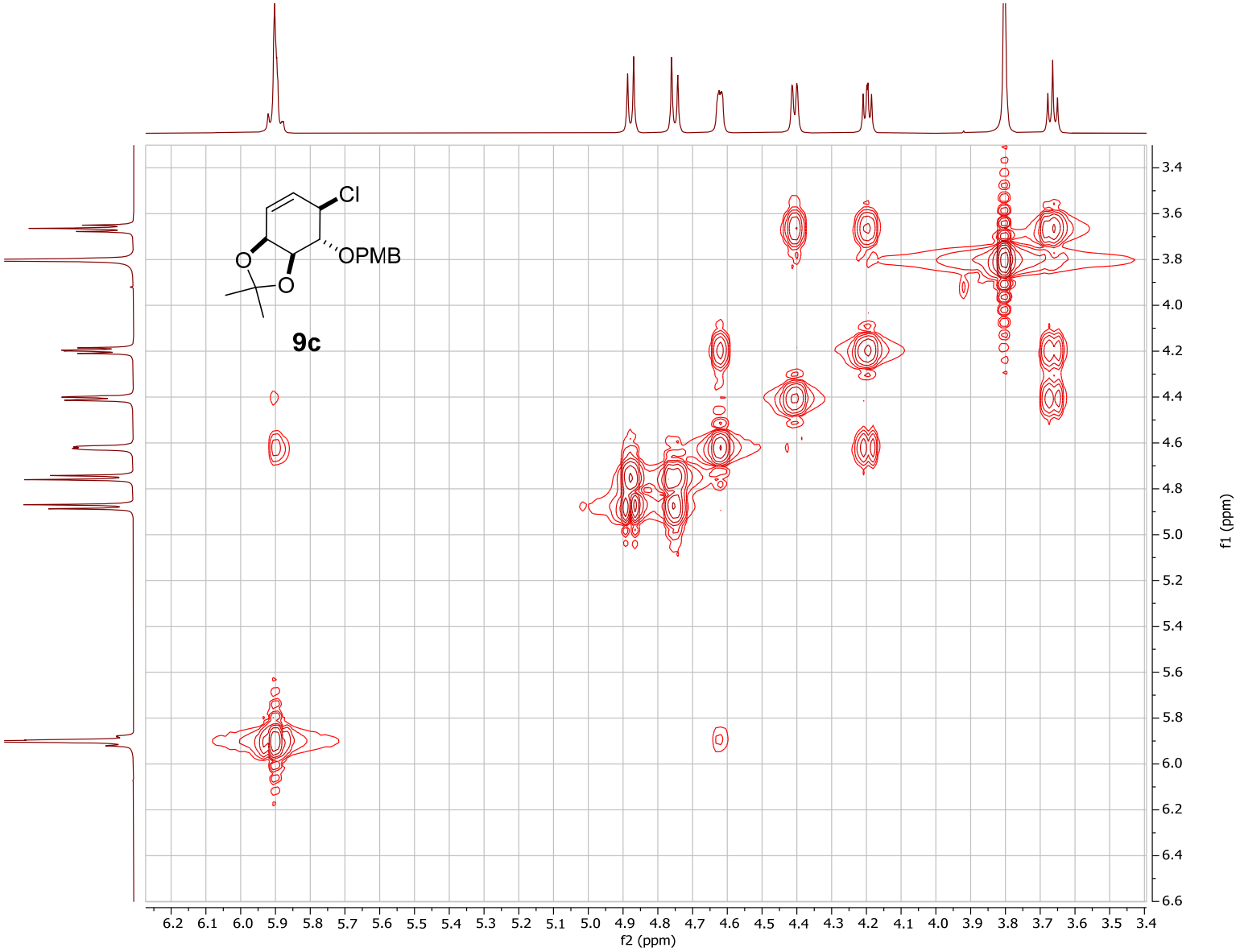


Figure S41: HSQC NMR spectrum of **9a** in $CDCl_3$.

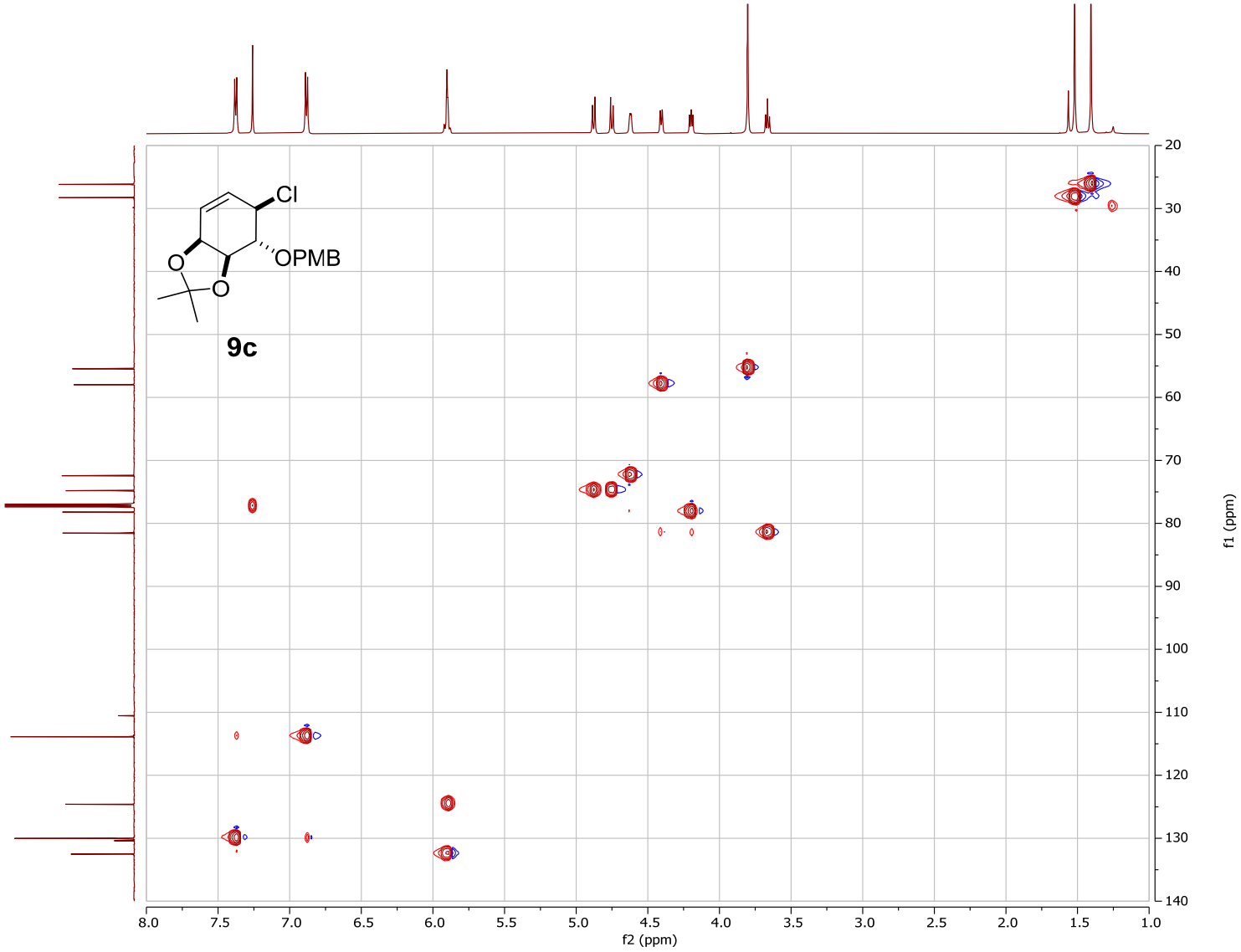


Figure S42: ^{1}H-NMR spectrum of inseparable mixture of **9b** and **9d** in $CDCl_3$ (600 MHz).

